Centrifuge Pellet Injector for JET

C. Andelfinger, E. Buchelt, D. Jacobi,
E. Lackner, H.B. Schilling, M. Ulrich,
G. Weber

IPP 1/218 August 1983

MAX-PLANCK-INSTITUT FÜR PLASMAPHYSIK

8046 GARCHING BEI MÜNCHEN

MAX-PLANCK-INSTITUT FÜR PLASMAPHYSIK

GARCHING BEI MÜNCHEN

Centrifuge Pellet Injector for JET

C. Andelfinger, E. Buchelt, D. Jacobi,
E. Lackner, H.B. Schilling, M. Ulrich,
G. Weber

IPP 1/218 August 1983

Die nachstehende Arbeit wurde im Rahmen des Vertrages zwischen dem Max-Planck-Institut für Plasmaphysik und der Europäischen Atomgemeinschaft über die Zusammenarbeit auf dem Gebiete der Plasmaphysik durchgeführt.

IPP 1/218 C. Andelfinger, E. Buchelt, D. Jacobi, E. Lackner, H.B. Schilling, M. Ulrich, G. Weber

Centrifuge Pellet Injector for JET

Abstract

An engineering design of a centrifuge pellet injector for JET is reported as part of the Phase I contract number JE 2/9016. A rather detailed design is presented for the mechanical and electronic features. Stress calculations, dynamic behaviour and life estimates are considered. The interfaces to the JET vacuum system and CODAS are discussed. Proposals for the pellet diagnostics (velocity, mass and shape) are presented.

Content

Figure captions

1. Introduction

A centrifuge pellet injector could serve as a device for quasi-stationary refuelling in fusion experiments. In the present state of the art pellet velocities of $\sim$ 2000 m/s seem possible from the point of view of tensile stresses in the centrifuge rotor. It is still an open question whether cryogenic deuterium pellets will survive the acceleration process. The compulsive acceleration reaches the order of 1×10^7 m/s^2. The pellets survive in smaller experiments with values of the order of $1 - 2 \times 10^6$ m/s^2. Full-size experiments are planned in a few months with the test facility under construction at Garching. A further open question is the final size of the pellets and their penetration into the plasma. The size will depend on the compatibility with the plasma, limited by the initiation of disruptions. The penetration depends, on the one hand, on the size and, on the other, on the energy distribution of the plasma particles. No experience is yet available on tokamak plasmas with strong additional heating. The ablation models can only be considered as rough estimates. Pellet injection with a pneumatic pellet gun, also part of the above-mentioned contract, which should be applied beforehand to the JET plasma, should deliver more reliable information.

For the technical solution of the centrifuge design the safety aspect calls for application of modern compound material for the rotor. With unidirectional carbon fibre compound rotor arms the moment of inertia and hence the stored kinetic energy could be minimized to a value of 125×10^3 joules.

A further critical feature will be the stray angle of the pellets. The acceptance of the port on a main horizontal flange will be $\pm$ 2.3 degrees. With smaller centrifuges and different pellet feed-in a stray angle of about $\pm$ 2 degrees was measured at Oak Ridge as well as at Garching. This point, too, can only be clarified with full-size test equipment.

2. Specification of requirements

Pellet size:

In tokamak experiments with pellet injection safe operation without disruptions was possible with pellet sizes of up to 100% of the plasma fuel. For periodic refuelling we should like to stay well on the safe side, which means that the pellet size should correspond to 20 to 40% of the fuel. For cylindrical pellets with d = h the pellet diameter would be about 2.3 to 3.0 mm for a total fuel of 4×10^{21} atoms.

Pellet velocity and penetration:

The maximum pellet velocity of 1600 m/s known at present is obtained in the Garching prototype gas gun. With the restrictions mentioned in the introduction, the penetration in a plasma with temperature and density profiles corresponding to the following equations may be estimated with the neutral shielding model for various velocities:

$$n_e = 8 \times 10^{19} \left[1 - (r/a)^8\right] + 2 \times 10^{19} \left[m^{-3}\right]$$

$$T_e = 6 \times 10^3 \left[1 - (r/a)^2\right]^{2.5} + 50 \quad \left[eV\right]$$

Figures 1 and 2 show the calculated particle deposition, density and temperature profile for d_{pellet} = 2.3 and 3 mm for velocities of up to 2000 m/s (in steps of 400 m/s).

Pellet frequencies:

In the hot plasma regime a particle confinement time of about one second can be expected. This calls for a pellet frequency of 5 Hz in the case of 20% pellets and 2.5 Hz in the case of 40% pellets. To cover also the case where the particle confinement time is essentially smaller, a maximum pellet frequency of 30 Hz is envisaged. The storage cryostat for the deuterium pellets has a capacity of 55 for the smaller and 40 for the bigger pellets. Quasistationary refuelling for about 10 to 15 s would therefore be possible.

Table I

Refuelling ratio $\frac{N_{pellet}}{N_{plasma}}$	20 %	40 %
Pellet size (d = h) (mm)	2.3	3
D_2 pellet mass (mg)	1.9	4.2
Stored pellet number	55	40
Proposed frequency (Hz)	5	2.5
Injection period (s)	11	16

3. Engineering design

The engineering design is governed by the following conditions:

- The centrifuge should be compatible with the requirements of the active phase operation.
- The vacuum conditions have to meet the needs of a category 3 diagnostic with an auxiliary pumping system. The centrifuge system has to be separated from the torus by an absolute valve and a quick-closing valve.
- It is assumed that difficult repair or maintenance can be done in the hot cell. Disconnection of all lines is envisaged in remote-handling technique conforming to JET standards. Exchange of vacuum pumps (JET standard) can be done by remote handling.
- All auxiliary systems, such as deuterium supply, liquid helium control, electronics and others, should be installed in the basement and the diagnostic area (South West Wing).
- All operations are remotely controlled via CODAS and activated with Edwards controllers and Simatic S5-150 modules.

3.1 Vacuum system

The vacuum system consists of a stainless-steel vacuum vessel with a burst protection ring inside, 2 JET standard turbomolecular pumps (TPU 510A), one small (40 l/s) turbomolecular pump connected to the intervening space between the rotor drive and centrifuge vessel. The two TPU 510A pumps in parallel are necessary to regain a good vacuum for cryostat insulation fast enough in the event of an accelerated pellet hitting a wall and evaporating. For controlling, JET standard branch pipe units together with Edwards controllers 2001 will be applied. The deuterium cryostats will be mounted on the cover of the vacuum vessel and will act in themselves as a cryogenic pump. Clean operation is imperative, otherwise these cryostats will be overloaded with impurities, which will impair deuterium pellet production. Figure 3 shows a scheme of the vacuum system. Details are described in the following sections.

3.1.1 Vacuum vessel

The vacuum vessel, which accommodates the centrifuge rotor, consists of a flat can with an inner diameter of 1000 mm and a vertical clearance of 200 mm. A 25 mm thick burst protection ring with an inner diameter of 905 mm is placed inside. The circumference of the vessel has

2 ports for the turbomolecular pump with remote-handling flanges with DN 150

1 port for a branch pipe unit I with remote-handling flange with DN 65

1 exit port for the pellets with DN 100 CF.

The big flange for the cover of the vessel will have an outer diameter of 1200 mm and will be designed closely in keeping with the JET standard remote-handling flanges with a double sealing helicoflex seal. The cover contains 4 radiation-resistant glass windows with DN 150 CF for diagnostic accessories.
There is a rotatable flange with DN 350 CF, on which the deuterium croystats and the feed-in mechanism will be mounted.

The centrifuge drive with a DN 250 CF flange will be mounted on the bottom. The connection for a small turbomolecular pump (Pfeiffer TPU 040) and measuring gauges will be integrated in this flange. The purpose of this is to maintain the vacuum in the feed-through of the rotor axis. In addition, a cooling baffle can be envisaged if necessary to prevent lubrication oil from entering the main vessel. Near the exit port will be a further diagnostic port with DN 150 CF. The total weight of the vessel with its accessories will be about 650 kg. All material will have a magnetic permeability of $\mu \leq 1.05$ (see material list). The main dimensions are given in Fig. 4.

3.1.2 Vacuum interface to torus vacuum system

The interface line to the JET torus vacuum system will be the main horizontal port flange of octant II. For the centrifuge pellet injector an all-metal valve supplied by VAT that conforms to

JET standard, series 43 DN 250, with JET remote-handling flange will be needed for separation of the pellet system. A double-walled bellows will decouple the pellet injection system from the movements of the main port flange during bake-out or disruptions. Slight bending of the pellet beam tube with reference to the original direction of the flange port axis is also needed to give clearance at the inner edge of the port at an expected stray angle of $\pm$ 3 degrees.

A ceramic break in series with the bellows part for electrical separation will be proposed.

This is followed by a fast valve which will open the centrifuge system during operation only while pellet injection is taking place. The interspace between the two valves will be pumped down by the centrifuge vacuum system to a pressure level lower than the torus vacuum. The opening of the separation valve will be controlled by CODAS via pressure gauges on both sides of the valve. V2 in Fig. 3 can be opened with atmospheric pressure in the interspace. The opening and closing times are about 20 ms. The life of V2 will be 20,000 closures. The pressure control will be done by JET standard branch pipe units I and Edwards controller 2001. Figure 5 shows this vacuum interface.

The interface to the JET backing line will be VAT angle valves DN 35 and CN 16, series 40, with JET standard remote-handling flanges. An alternative option may be to combine all forevacuum connections of the UHV pumps to one VAT valve followed by a bellows, a ceramic break and the backing line.

The ventilation line connected with the main turbomolecular pump via VAT angle vales CN 10, series 40, must be supplied with helium. Heavier gases will be frozen in the deuterium cryostats. Return to service would take long evacuation times.

The surface treatment of all inner surfaces will be carried out in conformity with JET quality document JET QUA 108.
Baking should be done with the following temperature distribution: V_1, torus vacuum valve, 250° C; V_2, fast shutter, 150° C; centrifuge vessel about 100° C.

3.1.3 List of pumps, valves and gauges

In the following all JET standard vacuum components outlined in Fig. 3 are listed.

Item number	type	manufacturer
P1	TPU 510	Pfeiffer
P2	TPU 510	Pfeiffer
V1	DN 250, series 43	VAT
V3	DN 35, series 40	VAT
V4	DN 35, series 40	VAT
V5	DN 16, series 40	VAT
V7	DN 10, series 40	VAT
V8	DN 10, series 40	VAT
BPU I_1	mounted on main port flange	
BPU I_{2-4}		Leybold-Heraeus
BPU III		Leybold-Heraeus
Pe1-4	Penning gauge	
Pi1,2,3,7	Pirani gauge	

Non-standard component:

P3	TPU 040	Pfeiffer
V2	fast closing valve	CETEC AG

3.1.4 Support structure

The support structure will be divided in height for practical reasons. During assembling and testing a height of the order of one metre for the pellet beam tube seems reasonable. At the JET site this will be about 6 metres.

This calls for a platform with the dimensions:

H = 4950 mm

B = 2 x 1000 mm

L = 2100 mm.

This platform consists of two towers designed as a lattice construction. For the support of the pellet gas gun the two towers are one after the other; for the centrifuge the towers are side by side.

The platforms only support the pellet injectors themselves and a 100 litre storage tank for the liquid helium. In the active phase of JET this tank acts as a buffer in the liquid helium service line.

The low support structure of the centrifuge has a hexagonal ground plane with jibs for the UHV pumps and the pellet beam tube. The ground frame has adjusting screws for proper alignment.
The basic design can be seen in Fig. 6.
The admissible load would be several tons. The arrangement will be oversized for rigidity. The proposed material is aliminium-base alloy.

3.1.5 Material list

Vaccum vessel:	stainless steel DIN 1.4311 or 4301
Burst protection ring:	stainless steel DIN 1.4311 or 4301
Rotor hub:	Al2nMgCu 1.5 F50 conforming to DIN 3.4365.71; about 0.6 kg
Rotor arms:	carbon fibre compound (Torayca T 400) fibre fraction 65%, about 0.6 kg
Cryostats:	electrolytic copper plated with gold stainless steel, DIN 1.4311
Ceramic break:	stainless steel, DIN 1.4301 Vacon 70, NiCo 2823, DIN 1.3982 Alumina V96, bellows DIN 1.4541
Beam line:	stainless steel, DIN 1.4311 bellows DIN 1.4541 or 1.4311
Support structure:	AlMgSi 0.5 F 22 DIN 3.3206.71

3.1.6 Vacuum control

The vacuum control system will be very similar to the system of the pneumatic pellet injector. For this reason the same numbering was applied in Fig. 3, but some components can be omitted for the centrifuge. In any case the centrifuge injector will be used after the pneumatic injector, it being possible to use the same hardware with a few modifications in the wiring.

The vacuum system is controlled by two Edwards 2001 controllers (see Fig. 7 /1-4). The first (EA) is used to handle the Pennings Pe1, Pe2, the Piranis Pi1, Pi2, Pi7 and the valves V1, V2, V7 and V8.
The second (EB) handles Pe3, Pe4, Pi3, V3, V4, V5 and P1, P2, P3.
The vacuum readings of the gauges are passed to CODAS via analog outputs of the gauge modules and a 16-channel A/D-CAMAC module (Fig. 7/1-3). The A/D module is also used to monitor the baking temperature (Fig. 7 /3). The connections of the input and output units are given by the following notation: connected device (high-level signal/low-level signal). The JET valve V1 is operated by CODAS and CISS. Request signals to operate V1 are provided by EA U1 Ch1-2. A feedback signal of V1 is provided by CODAS via LSD output on EA U2 Ch1. A request by the operator to close V1 (EA U6 Ch2) is always passed to CODAS, a request to open V1 (EA U6 Ch1) only if Pe2 < Pe1. If Pe1 is high, close V1 will be requested without operator interference.
"Close V1 by CISS"(EA U5 Ch6) will be requested if V2 fails to react on close command.
The fast valve V2 is controlled by EA U1 Ch3 in all operational phases except when the vacuum system is ready for pellet shots. In this case the control of V2 is passed to the Simatic control system by EA U1 Ch4. When under Edwards control V2 is always opened if V1 is closed and vice versa.
The desired mode of operation (vacuum system on/off, manual/automatic

operation) is received by EA U4 Ch6-7. In the"off"state the power of all units, except V1 or V2 (one of which remains opened),is switched off. If the "off" state has been reached by a shutdown procedure initiated by a failure of certain components,elusive fault alarms will be given (EA U3 Ch3-5, EA U5 Ch5, EB U3 Ch1-3). The"off" state can only be left if a reset pulse (EA U4 Ch4) is given which also resets the elusive fault alarms. The vacuum system "on" state will only be reached if Pi7 is low and all cooling water circuits (EA U2 Ch8, EA U4 Ch1-2) are operating after the water supply is switched on. A failure of the backing pressure, cooling system or pumps returns the system to the"off" state (through different shutdown procedures). The actual operation mode is passed on to the operator (EA U3 Ch7-8, EA U5 Ch4, EA U5 Ch7) and information on the operation mode is exchanged between the controllers (EA U4 Ch5, EA U5 Ch1-3, EA U6 Ch3).

After a valid"vacuum on command"EB opens V3-V5 and switches on P1-P3 (EB U1 Ch2-7) if Pi3 is low. When Pe3-Pe4 are low,EB U1 Ch1 gives a signal to EA. EA reacts by passing control of V2 to Simatic and issuing a "ready for shot" signal (EA U5 Ch4) if V1 is opened. The system returns to the "not ready "state as long as either of Pe3-Pe4 is high (e.g. after each shot).

A shutdown procedure will be initiated by failure of the backing pressure or of the cooling water circuits (initiated by EA) or by failure of P1-P3 (initiated by EB). Two different shutdown procedures will be executed,depending upon the state of the cryostat (EB U6 Ch6). If the cryostat is warm,all connected units of EA and EB are immediately de-energized. If the cryostat is cold, V5 remains open and a signal (EB U3 Ch4) is given to EA to inhibit the opening of the gas admit valves V7-V8. The worst case of shutdown with cold cryostat and failure of the backing pressure or power failure is handled by a passive excess-pressure valve.
In the "vacuum on "state the system may be switched to manual control of V3-V5 and P1-P3 (especially to investigate minor faults). The state of these elements is maintained during the transition

unless EB U4 Ch2-8 or EB U6 Ch1-5 are operated. The control of major failures remains active in the manual mode. Feedback signals of all valves and pumps are passed to the controllers and to LSD ports (Figure 7/2,4, bottom) for the information of the operator.

List of hardware

2 Edwards 2001 controllers
4 Penning modules (total number)
2 Pirani modules (total number)
8 I/O modules (total number)
8 Relay output/opto input units
(1 spare unit for each controller allowing small changes of concept are included)
1 Amplifier for PT 100
(CAMAC and LSD components are listed separately).

3.2 Centrifuge rotor

As proposed in the conceptual design, the shape of the straight arms was established for the rotor geometry.
For the approximation $r_o << R$ the pellet velocity becomes $v_r = v_t$:

$$V_{pellet} = \sqrt{V_r^2 + V_t^2} = 2\sqrt{2}\pi f R$$
$$V_{pellet} = 1600 \text{ m/s for } 400 \text{ Hz and } R = 450 \text{ mm.}$$

The acceleration angle $\varphi = \omega t$ is obtained from

$$\frac{2R}{r_o} = e^{\varphi} + e^{-\varphi} \quad \text{for } r_o = 35 \text{ mm}, R = 450 \text{ mm and } \dot{r}_o = o$$

$$\varphi = 186^o.$$

The Coriolis acceleration reacting on the rotor while a pellet is being accelerated will be highest at the outmost radius

$$b_c = 8\pi^2 f^2 R$$
$$b_c = 5.7 \times 10^6 \text{ m/s}^2.$$

This Coriolis acceleration excites the rotor arm to bending oscillations. Excitation is highest near the end of acceleration. With the biggest possible pellets (about 100% of the fuel) with a mass of 10 mg, the maximum force will be

$$F_{max} = m_p b_c = 10^{-5} \times 5.7 \times 10^6 = 57 \text{ N}.$$

The pressure acting on the pellets during acceleration will be of the order of a few 10^6 Pa $\hat{=}$ 10^{-1} kp/mm^2. For this value there is uncertainty because the contact area is unknown.

In our test setup with a Beckmann centrifuge drive model L8-55 preliminary experiments were conducted for speeding up single arm rotors. Only rotors with relative heavy hub could be brought through resonance at low frequencies. But rotors with two arms crossed at an angle of 90 degrees have had no difficulties in crossing these resonances. Calculations confirmed what was found experimentally.
With this knowledge, the final design for the rotor was done by MAN-Neue Technologie, accompanied by stress calculations and considerations of the dynamic behaviour of the rotor.

The limitation to a revolution frequency of 400 Hz was not made because of tensile stresses, but rather because of limitations of elastic elongation to below 0.7% for the compound material. This value was recommended by a firm with expertise in the design of ultra centrifuges. In fact, we do not need a constant frequency, since we can reduce the frequency in between the pulses to lower values, thus reducing the effect of stretching the epoxy. From the point of view of strength there is a good chance of reaching 500 Hz or a pellet velocity of 2000 m/s.

3.2.1 Mechanical design

A detailed mechanical design was made and the manufacturing of two rotors for the test setup is in progress. Figure 8 (assembly drawing SK796 C) shows the features. The rotor hub consists of a lower and upper rod suspension for the two CFC arms. These arms can be independently adjusted by pressing the plate springs, which

hold the arms in position. The design is completely symmetric to the rotation axis except for the pellet feed-in guiding tube. This tube guides the pellets to the acceleration groove of the CFC arm, which will be approximately matched to the pellet diameter.

The imbalance of the complete rotor, its weight being about 1.2 kg should be $\leq$ 3 gmm.

Figures 9 to 11 show detailed drawings of the upper and lower rod suspension and the CFC arm. A complete set of drawings has been submitted to JET (see drawing list).

The physical properties of the materials are given in the following list:

Rotor hub: AlZnMgCu 1.5 F50 age-hardening
density 2.8 g/cm^3
E module 70,730 N/mm^3
tensile strength 510 N/mm^2
0.2 elastic limit 450 N/mm^2

Rotor arm: "Torayca T 400" carbon fibre
density 1.74 g/cm^3
E module 240,000 N/mm^2
compound material (65% fibres)
density 1.55 g/cm^3
E module // 1.56 x 10^5 N/mm^2
bending module 1.3 x 10^5 N/mm^2
tensile strength // 2730 N/mm^2 normally
min. 2450 N/mm^2.

3.2.2 Stress considerations

Stress calculations for the designed centrifuge rotor were carried out by MAN-Neue Technologie and presented in report No. MAN A 190 128-EGS-001, submitted to JET. The assumptions for the calculations are:

rotor frequency:	400 Hz
pulse cycle A	pellet frequency 30 Hz; 50 pellets and a pellet mass of 2.5 mg
pulse cycle B	pellet frequency 30 Hz; 30 pellets and a pellet mass of 10 mg
desirable number of cycles A or B	10,000.

The essential results are:

- max. tensile stress in the middle of the rotor arm due to centrifugal force

$$\sigma_{max} = 991 \text{ N/mm}^2.$$

- Bending stress will be produced by the pellets during acceleration as a result of Coriolis forces. As mentioned above, the force acting tangentially will be

$$F(t) = 2\, m_{pellet}\, r_o\, \omega^2\, e^{\omega t}$$

This force increases exponentially and attains its max. value at the end of acceleration.
Such an impact is about equivalent to a uniform loading at the end of the rotor arm with F = 57 N and a time interval of $\Delta t = 0.6$ ms. The relation of this time over the period of the rotor arm resonance frequency $\Delta t/T \approx 0.24$ results in a dynamic load factor DLF = 1.4 (from "Structural Design for Dynamic Loads", McGraw-Hill Book Comp. 1959).
This makes the dynamic deflection of the arm

$$x_{dyn} = 1.4\ x_{stat}$$

which will effect a <u>bending stress</u> in the edge fibres of the arm of

$$\sigma_{b\,max} = \frac{M_{by}\ s_{dyn}}{J_y} = \frac{35910 \times 10}{4496} = 80 \text{ N/mm}^2.$$

Owing to the pellet load there is also a bending moment on the elastic rotor shaft which causes an additional bending stress of 4 N/mm^2.

The total tensile stress on the rotor arm is the sum of the values due to centrifugal forces and pellet load:

$$\sigma_{total} = \sigma_{\parallel max} = 991 + 80 + 4 = 1075\ N/mm^2$$

this being rather small compared with the breaking stress of the compound material with $\sigma_{\parallel} \approx 2700\ N/mm^2$.

For estimating the working life as a function of the variable load with time the static load of the centrifugal force does not matter. The rotor arm resonance frequency will be excited by the impact of the pellet. With a resonance frequency of about 500 Hz, a pellet frequency of 30 Hz and 50 pellets per cycle the load cycle becomes for 10^4 cycles

$$n = \frac{500}{30} \times 50 \times 10^4 = 8.3 \times 10^6.$$

The decrement δ of the oscillation is listed by the manufacturer of the material as a function of the frequency. With f = 5oo Hz δ becomes $\delta = 0.004$, which gives rather small damping between the pellets. We can assume a constant stress amplitude.
Figure 12 shows the life characteristic for a load cycle of 10^7 (Breutmann, L.J.,Krock, R.H. Composite Materials, Vol. 5: Fracture and Fatigue). A and B denote two possible loads.
The points are very distant to the life characteristic and we can expect that the rotor arm will survive a sufficient number of load cycles.

The rotor hub will be much less loaded. The max. stresses in the hub components are all smaller than $\sigma_{max_2} < 76\ N/mm^2$, and thus very small compared with $\sigma_{0.2} = 450\ N/mm^2$.

The stress concentration factors are all below $\alpha_k \leq 3.9$. With these numbers we get from the life characteristic of the proposed material possible load cycles of $n > 2 \times 10^6$. In reality we estimate numbers for acceleration and deceleration of the rotor of a few times 10^4. Details are given in the above-mentioned MAN report.

3.2.3 Dynamics of the centrifuge rotor

A detailed description is presented in the MAN-Neue Technologie report No. A 190 128-EDS-001. For dynamic calculations the centrifuge is regarded as a rigid rotor on a flexible shaft. This gyroscope model has four important bending eigenvalues: double motion of precession and of nutation as shown in Fig. 13.
The two major problems are oscillations and oscillation damping while the rotor is speeding up and those caused by the acceleration of a sequence of pellets.

Oscillations during speeding up the rotor

With rising rotor frequency three eigenvalues are crossed, but since only ^{+}P rises with rotor frequency this is the only resonant crossing. As shown in the diagram (f_{eigen} vs f_{rotor}), the critical speed of rotation has to be overcome at a rotor frequency of about 30 Hz.
From measurements at the test setup a phase angle $\delta = 8^{o}$ between the force and displacement amplitudes was calculated. This damping value will limit the displacement amplitude of the rotor to 1 mm if the existing imbalance is 40 gmm. Since the imbalance probably can be kept as low as 2 gmm, the maximum displacement amplitude will only be 0.05 mm.

Oscillations induced by pellet acceleration

Three different types of oscillations are considered.
Bending oscillations of the CFC rotor arm was discussed in the stress considerations.
Torsional oscillation frequency was calculated to be 86 Hz and evaluation for the torsion angle gives $\varphi = 0.00145^{o}$. This is equivalent to s = 0.0114 mm at the end of the rotor arm and shows so weak an excitation of torsional oscillations that it need not be considered any further.
Bending oscillations of the rotor shaft are excited by the force acting on the rotor arm during pellet acceleration. The reaction of the gyroscope to that disturbance are oscillations dominated by the eigenvalues $\pm$ P (both about 40 Hz) and -N (0.11 Hz); The eigenvalue +N (795 Hz) is not excited.

Figure 14 shows two typical patterns of rotor excursion for a series of 50 pellets (10 mg each). In the upper diagram the pellet frequency is 40 Hz and excitation of oscillations is in phase with $\pm$P, while in the lower diagram the pellet frequency is 27 Hz and excitation is therefore out of phase with $\pm$P. The low-frequency component -N (0.11 Hz) is excited by every pellet in both diagrams, owing to the long period of -N oscillation (8.85 s).

Even amplitudes of about 1 mm would have no essential influence on the stray angle of the pellets, their contribution being less than 0.13 degree.

3.2.4 Rotor drive

The drive system now used in the test centrifuge is based on the Beckmann L 8 centrifuge drive. Since the L 8 system is not intended for remote operation, interfacing to CODAS would be rather difficult. It is therefore proposed that an advanced model (LA 8M) with a serial (RS 232) interface be used. The system (see Fig. 15) is connected to a direct-drive induction motor which is frequency-controlled and water-cooled (2 l/s). Its maximum speed is 50,000 rpm. The time necessary to speed up the rotor to 24,000 rpm will be several minutes. To prevent unsafe operation, there are interlocks controlled by a vacuum gauge, an imbalance switch, drive temperature and an overspeed sensor. A disc on the drive spindle with reflecting and non-reflecting sectors in conjunction with a reflex light barrier is used to control the drive speed. A similar disc on the rotor hub is used for overspeed and rotor angle detection. For radiological reasons quartz fibres are used for light signal transmission between the centrifuge in the torus hall and control electronics in the basement.

The desired operating conditions (rotor speed, holding time) are transferred from a serial input/output CAMAC module (CTR3) to the serial port of the centrifuge controller. The proper coding of the serial signals is generated by an auxiliary crate controller (CAC).

The centrifuge speed is evaluated by counting the output pulses of the overspeed sensor (60 pulses per revolution) with a latching scaler (CCT4) during the counting intervals of 1 s produced by a continuous clock-pulse generator. The centrifuge frequency is also a good measure of the velocity of the accelerated pellets. The output of the overspeed sensor together with a 1 pulse per revolution signal is also used for the pellet feed-in synchronization (Sec. 3.42) to detect the momentary rotor angle. The serial interface signals and the rotor speed signals are galvanically decoupled by digital opto-couplers. Feedback signals of the interlock conditions and the switches for the centrifuge power and cooling water control and feedback are handled by LSD connections.

List of hardware

1 Centrifuge drive and control unit (Beckmann LA 8M)
3 Digital opto-couplers (to be determined)
1 Clock-pulse generator (to be determined)
(CAMAC and LSD components are listed separately).

3.3 Pellet cryostats

The cryogenic system consists of three main components:

- the helium supply
- the extrusion cryostat
- the storage cryostat.

In the non-active phase of JET it is proposed that both cryostats be supplied with liquid helium from a 100 l tank via siphon pipes. The gaseous helium exhaust will be returned by an exhaust line to the liquid helium facility. In the active phase the tank should be permanently connected with a JET standard liquid helium line. The helium will be pumped through the cryostats with the help of Leybold-Heraeus helium-tight rotary vane pumps of type D16A.

The extrusion cryostat will be a commercial Leybold-Heraeus unit with increased storage volume of 1500 mm^3. It serves for production of the frozen deuterium and dispensing of the solid deuterium rod, from which the pellets are cut.

The storage cryostat stores the mentioned deuterium rod and contains the mechanism for transporting the rod through the cutting device.
Figure 16 shows a scheme of the cryogenic system.

3.3.1 Extrusion cryostat

Figure 17 shows a drawing of the Leybold-Heraeus extrusion cryostat. The deuterium enters the cryostat through the D_2 pipe, which will be cooled by the helium exhaust. To freeze the deuterium in the storage volume, the cryostat temperature will be lowered to 6 K. For the extrusion the temperature will be increased to 8.5 - 9 K with the help of an electric heater. Then the extrusion piston will be moved by a hydraulic actuator. The pressure acting on the frozen deuterium will be about 15 MPa, which is high enough to extrude the deuterium through an exchangeable nozzle. Its diameter determines the diameter of the pellets.

If the extrusion velocity is limited to less than 2 cm/s,the deuterium rod will have a homogeneous appearance, without cracks in the surface.

Figure 18 shows a photograph of such deuterium rods. Below the extrusion nozzle the storage cryostat is mounted in line with the extrusion axis. The storage cryostat will be loaded during extrusion.

3.3.2 Storage cryostat

The storage cryostat as shwon in Fig. 19 has to be thermally insulated from the extrusion cryostat and should have a constant operation temperature of about 5 K, adjustable with the helium vapour pressure control circuit. The temperature determines the brittleness of the deuterium rod and may influence the stray angle of the pellets produced by the cutting of the rod.
The storage cryostat is in the shape of a quarter-circle with a radius of 8 cm. Tests have shown that the rod could be bent to this shape without damage. The bent length is 125 mm, delivering about 40 pellets with a length of 3 mm.

3.3.3 Cryostat control

To start operation of the cryostat, the following requirements must be met:

- The vacuum in the centrifuge vessel must be $< 10^{-5}$ mb,
- the deuterium pipe must be evacuated and flushed with deuterium, and
- a revertive signal of the deuterium and liquid helium supply has to indicate a sufficient supply.

The complete system will be controlled by Simatic S5-150. The cooling down of the cryostats and the first filling up will be manually initiated by the operator by remote control. Normal operation during the experimental phase will be done automatically by the Simatic, but timed by the clock signal from CODAS.
The procedure which has to be done by the Simatic will be:

- Control of the above-mentioned requirements.

Procedure for cooling down the cryostats:

1) helium exhaust pumps "on"
2) helium exhaust heater "on" (rated temperature 20^{o} C)
3) membrane gauge fully "open"
4) siphon valves for controlling the helium throughput fully "open". The He exhaust pressure should be 200 - 250 mb.

The cooling down phase will last about 90 min. The cryostat temperatures are measured with a resistance thermometer (carbon resistor 100 Ω) and with He vapour pressure gauges.

Procedure for deuterium rod production:

1) closing of slide valve between extrusion and storage cryostats (rod transport arm in cutting position)
2) adjustment of temperature to 6 K with HR3 control unit
3) opening of deuterium pipe, flux limitation to 300 Nccm/min, p = 500 mb, lasting about 1 min
4) stopping of deuterium flux and compression of the frozen deuterium with p $\approx$ 15 MPa. (3) and (4) have to be repeated until the storage volume of the extrusion cryostat is filled to 90%. Normally 3 cycles are needed

5) retraction of the slide valve (transport arm) for opening the extrusion channel
6) lowering of the extrusion piston without pressure
7) increasing of the extrusion cryostat temperature to 8.5 K with programmed HR3 control unit
8) activation of the piston with an extrusion pressure of 15 MPa. The piston stroke is controlled and determines the length of the deuterium rod
9) inactivation of the piston
10) decreasing of the temperature to $\approx$ 5 K
11) transport arm cuts the rod in the slit between the two cryostats. The system is now ready for charging the centrifuge pellets.

Figure 20 illustrates the flow chart of the Simatic for the operations listed.

3.3.4 Pellet gas supply

The gas supply for pellet production in the cryostat will be the same for the gas gun and centrifuge injector. Besides the main pellet materials, deuterium or hydrogen, other gases, but with a preference for neon, are available for producing doped pellets. This will be more important for diagnostic work involving the pneumatic pellet injector.

The gas supply system should be located in the basement, so as to avoid remote handling, but operation will be done by remote control. The amount of stored gas should be high enough, so that during the active phase the bottles only rarely have to be exchanged. The exchange can be done without ventilation of the complete system. Quick connections are envisaged for piping. Figure 21 shows the scheme of the gas supply. The gas mixture in V5 will be CODAS-controlled by controlling the pressures in the volumes V1 - V4 by means of motor-controlled pressure regulators. The interface to CODAS will be handled with the CAMAC modules.

The mixture system in the basement is connected by only one gas feed line with the pellet cryostat in the torus hall. A very clean gas will be necessary for operation. Small admixtures of air, water or oil will already prevent proper pellet production.

Removal of all unwanted impurities will be done by evacuating the approximately 15 m long transfer line from both sides and by flushing with hydrogen.

The typical operating pressure in the line will be several hundred millibar.
Figure 22 gives the flow chart for control of the fuel gas supply.

3.3.5 Liquid helium consumption

For approximately 90 min the cooling-down phase from 293 K to 6 K needs a helium gas flux of 30 l/min for the extrusion cryostat and 40 l/min for the storage cryostat. The corresponding liquid helium consumption will be about 9 l.

In the operation phase about 6.5 l/h will be consumed. A 100 l tank will become empty in an operation time of 10 - 12 hours. It cannot be exchanged during an experimental shift because the siphon pipe freezes in the cold state. For this reason we recommend a liquid helium service line.

3.4 Feed-in of pellets

An indirect feed-in process will be chosen for loading the centrifuge rotor with pellets. The deuterium rod stored in the cryostat will be pushed out with the required timing in steps of one pellet length. A cutter arm cuts the pellets and accelerates them in front of the entrance of the centrifuge rotor. This feed-in process must be properly synchronized with the rotor frequency.

Owing to the clearance needed between the rotor and feed-in mechanics the pellets have a flight path of 5 mm in a minimum rotor revolution time of 2 ms. This means the min. pellet velocity must be > 2.5 m/s.

A value of 3 m/s will therefore be desirable.

The cutting pulse could be derived from the rotor revolution in steps of 6 degrees, corresponding to 33 μs for 500 Hz or to a flight path of 0.1 mm. Besides the synchronization clearance, there are additional vertical and radial clearances of 0.25 mm and 0.35 mm, respectively. This allows a pellet speed fluctuation of about 4% and a radial stray angle of about $\pm$ 3.8 degree. A comparable stray angle in the azimuthal direction would cause a fractional stray angle at the pellet exit of about $\pm$ 0.6 degree, which would be acceptable.

3.4.1 Mechanics of pellet feed-in

As mentioned in Sec. 3.3.2, the pellet material will be stored in the quarter-cycle-shaped storage cryostat. Figure 23 shows a scheme of the mechanical arrangement. Ejection will be done by a rotating arm (90^{o}) whose front end is cooled by contact with the cryostat and whose hub is thermally insulated by a thin stainless-steel structure. The vacuum feedthrough is tightened with ferrofluids. The ejection arm is driven by a stepping motor with 0.5 mm steps. At the upper end position the arm can be withdrawn with the help of an elbow joint for opening the storage cryostat for refuelling. A cutting device is placed at the lower cryostat end.

The cutter has the shape of a rocker arm with a ladle which is matched to the pellet diameter and length. This ladle moves between a cutting edge and a stop dog, driven by a cam ring with 5 small ball bearings as cams with a keying ratio of 1 : 4. For a max. frequency of 50 Hz there is 16 ms time for deuterium rod feed. The cam ring runs continuously, only the light-weight ($\approx$2 g) rocker arm must be accelerated and decelerated. It is driven by a stepping motor and synchronized with the centrifuge rotor. The cutter mechanism will not be actively cooled because the dwell time of the pellets in the ladle will only be about 2 ms.

The final velocity of the pellets is determined by the slope of the cam arrangement.

3.4.2 Control and synchronization of pellet feed-in

The two stepping motors are driven by motor power controllers located in the basement. Their control inputs are connected via optocouplers to the motion controllers in the diagnostic area. The motion controller for the cutting device is initiated by a CAMAC timer (CTM1) to accelerate the cutter motor to a step frequency of 10 times the rotor frequency, which results in a cutting frequency of 1/10 of the rotor frequency. After acceleration the cutting time is phase-locked to the rotor angle. The desired rotor phase angle for cutting is set by a CAMAC I/0 module (CPR1) in steps of 6^{o}. The rotor phase angle is evaluated from the centrifuge frequency f_c and 60 f_c signals from the rotor drive. The cutting time is obtained by a coding disc mounted on the cam ring axis of the cutting device, which is sensed by a reflex light barrier via quartz fibres.

Two similar light barriers are used for the ejection arm to mark the end positions (arm withdrawn or end of ejection). The motion controller of the ejection system is connected to LSD outputs to accept signals to withdraw the arm or to return to the ejection position. Feedback signals (arm withdrawn, ready for ejection) are supplied to LSD inputs. The pellet ejection is initiated by another output of the timer. The conditions of the pellet burst (length of pellets, number of pause steps between two pellets, number of pellets) are set by another I/0 module. The ejection of each pellet is synchronized to start with the end of the preceding cutting pulse. When the arm reaches the end of the injection position, it is automatically withdrawn to allow a new filling.

List of hardware:

2 Stepping motors (Berger RDM 5913/50)
2 Motor power controller (Berger NI 3426)
2 Optocoupler cards (option to NI 3426)

3 Reflex light barriers (to be determined)
1 Ejector motion controller (to be developed)
1 Cutter motion controller (to be developed)
(CAMAC and LSD components are listed separately).

3.4.3 Further tests needed

As mentioned in the introduction, the successful operation of the designed centrifuge injector cannot be predicted. Numerous tests have to be made in a full-size test device which will be constructed by the end of 1983. After delivery of the rotors the successful crossing of resonances and acceleration to full nominal speed will have to be shown experimentally and a representative number of load cycles should be absolved.

The stray angle of the pellets caused by the cutting process has also to be measured in the cryostat test equipment. Besides this investigation, the lifetime of the feed-in mechanics operating in ultrahigh vacuum has to be determined. These experiments will be started in September 1983.

Finally, after ingetration of both test facilities, the survival of the pellets during acceleration and the stray angle after acceleration have to be investigated.

In the event of negative results in the above-mentioned tests, the construction of a centrifuge pellet injector should not be recommended. At a very rough estimate these investigations will take about one year from now. Figures 25 and 26 show photographs of the test equipment.

3.5 Pellet diagnostic

The pellet diagnostic will be limited to determining

- D_α emission on the pellet path in the plasma, looking through the pellet beam line;
- the pellet mass with the aid of a microwave interferometer;
- the pellet velocity, which will be taken from the circumferential velocity of the centrifuge;

- the pellet shape by a TV system. This system only serves as an aid for the operator and the data will not be transmitted to CODAS.

The pellet path in the plasma region is such that is is in the viewing angle of the vertical bolometer camera and the vertical soft X-ray diode array.

3.5.1 D_α diagnostic

D_α emission occurs during the ablation of the pellets. The intensities are therefore a relative measure of the particle deposition in the plasma, and the pulse duration in conjunction with the known pellet velocity yields the penetration depth.

In the beam tube a quartz prism will deflect the light through a vertical standard quartz window DN 35. The light will be transmitted via a quartz fibre cable to a diode installed in the basement for radiation protection.

The maximum ablation time will be of the order of 2 ms. Because the fine structure of the signal is of interest, a sampling rate of 100 kHz will be required with a repetition frequency of up to 30 Hz for a maximum of 50 pellets. Most parts of the required electronics for data acquisition and remote control could be taken from the "provisional soft X-ray diagnostic". Figures 27a to c show the electronic scheme and, in part, the detailed circuits. The required memory needs a capacity of 25 K words for an observation time of 5 ms after the trigger pulse from the pellet mass diagnostic.

The output of the detector diode is amplified by a preamplifier located close to the diode. An existing preamplifier from the provisional soft X-ray diagnostic (Fig. 27b) will be used. The gain of the preamplifier can be set by two relays which are operated by changing the power supply voltages. The diode and the preamplifier will be placed in an insulating cabinet. The main

amplifier (Fig. 27c) located in the local-unit cubicle will be connected to local ground. The low-bandwidth isolation amplifiers of the provisional soft X-ray diagnostic can therefore be omitted. The gain of the amplifier chain is determined by the setting of 6 LSD output bits. The output of the main amplifier is connected via an anti-aliasing filter to a CAMAC ADC module (CAD4) with an associated memory module (CME 4). The CAD 5 of the provisional soft X-ray diagnostic has to be replaced by CAD 4 owing to the 1 MHz sampling rate required for the pneumatic injector, which will be installed prior to the centrifuge.

Because of the lower resolution of the CAD 4 (10 bit) the bandwidth of the filter may be adjusted close to half of the sampling frequency. The leak current of the diode is compensated by a digital regulation circuit. A signal from the CAMAC timer (CTM1) is used to freeze in the leak compensation during the JET discharge. A defined leak current can be added for testing the amplifier chain. The leak current and the supply voltages are monitored by another CAMAC ADC (CAD1). A second regulation circuit is used for the bias voltage of the diode. The bias voltage is preset with the possibility of changing its value by ramp-up and down inputs. The diagnostic can also be tested by a light circuit to simulate the light input of the diode.

The data recording is initiated by a trigger pulse from the pellet mass diagnostic. For each trigger pulse the clock-pulse generator generates a burst of 500 clock pulses of 100 kHz. At the end of the JET pulse further data transfer is inhibited by a stop trigger pulse from the timer. The start signal for the timer is generated by the CTS and, in the case of pellet shots without JET discharge, by the Simatic control system.

List of hardware:

1 Detector diode (double diffusion silicon diode, Quantrad 5 x 20 PIN 300-MP)

1 Preamplifier (from soft X-ray diagnostic)

1 Main amplifier with power supplies and a test light source (from soft X-ray diagnostic)

1 Clock pulse generator (to be developed)

CAMAC and LSD components are listed separately.

3.5.2 Measurement of pellet mass

The pellet mass will be measured by means of a microwave interferometer. One branch of the interferometer waveguide crosses the pellet path in the entrance of the beam tube. The pellet mass is directly proportional to the phase shift, measured in the interferometer, i.e. proportional to the peak value of the differential signals of the diodes.

The applied wavelength will be 3 cm. For an assumed stray angle of the pellet, $\pm$ 2.3 degrees horizontally and $\pm$ 1 degree vertically, the waveguide needs a slit of about 55 mm in length and 7 mm in width. Figure 28 shows a scheme of the interferometer with its essential components.

The expected pulse width in the pellet velocity range of 1000 - 2000 m/s will be 10 - 5 µs. With the pellet sizes proposed for JET, the differential signal of the microwave detectors will be of the order of a few mV.

The accuracy of the method depends on the field distribution in the measuring region of the waveguide influenced by the slit and fractional reflections in the system. We assume that an accuracy of 10% should be possible.

The interferometer should be installed in the basement for radiological reasons. Only the measuring branch waveguide will enter the torus hall. The detector signals will be galvanically decoupled by an isolation amplifier and amplified to a level in

the volt range for transmission to the diagnostic area.
The data acquisition could be done in the following manner (see Figure 29):
The amplified signals first pass a bandpass filter to reject low and high-frequency noise. An analog gate operated by a CAMAC timer (CTM1) signal is used to suppress noise signals outside a suitable time window. A following trigger stage produces time reference signals for each pellet leaving the interferometer. These signals are used to

- store the time of pellet delivery
- trigger the D_α diagnostic
- trigger the TV system for pellet shape monitoring
- store the peak value of the interferometer signal.

The time of pellet delivery is recorded by a combination of a CAMAC latching scaler (CCT4) and memory (CME5). (The alternative use of a CAMAC stop watch is unfavourable owing to its low resolution of 16 bit and the restriction to 16 timing signals at each input.) The counting of the latching scaler is started from the timer by disabling the veto input of the scaler. The timer also passes the 1 MHz clock pulses of the CTS to the latching scaler. The time delays of the trigger pulses with respect to the start of the JET discharge are stored as two 16-bit words for each pulse. For pellet shots without JET discharge the start pulses must be generated by the Simatic control system. The pellet mass information can be obtained by using a fast peak value rectifier with a decay time of a few milliseconds to reduce the real-time problems. The rectifier output is connected to a CAMAC ADC (CAD2). The clock pulses for the storage of the peak values into a CAMAC memory (CME2) are generated by the trigger circuit. The ADC is initiated by a trigger signal from the timer simultaneously with the analog gate.

List of hardware

1 Isolating amplifier (to be developed)
1 Signal conditioning circuit (to be developed)
CAMAC and LSD modules are listed separately.

3.5.3 TV system for pellet shape monitoring

In addition to the pellet mass information obtained by the microwave interferometer, a TV recording system will be used to monitor the pellet shape. This system only serves to inform the operator and will not pass results to CODAS. The TV system will be the same for both the pneumatic and the centrifuge injector and can be maintained when replacing the pneumatic injector by the centrifuge. In order to avoid magnetic interference, a solid state camera will be used. (Either English Electric Valve P 4300 or Fairchild 3000 with European TV standard will be selected when information about the Fairchild camera is available.)
For the D-D phase only moderate shielding of the camera and an associated solid state laser will be necessary. This may be achieved by locating them behind a transformer limb using image-forming fibre optics for the camera and ordinary fibre optics for the laser. In the D-T phase periscope systems to the basement (to be developed) will be necessary to achieve adequate shielding. Both the camera and the laser have to be isolated from the experiment with the only ground connection at the local unit cubicle.

The TV system and its connection to CODAS is shown in Fig. 30. The power of the camera will only be switched on for a few seconds for each pellet shot in order to reduce the sensor temperature. In this way the image quality will be improved without active cooling measures. When the pellet has passed the pellet mass diagnostic, the laser is triggered to produce a shadow image of the pellet. Since the readout time of the sensor is 40 ms, laser pulses with closer spacing must be avoided. A circuit which disables trigger pulses for 40 ms after each valid trigger is used to inhibit double exposure. For pellet frequencies higher than 25 Hz part of the pellets will not be recorded but the remaining samples will be adequate to judge the average pellet quality. The method of recording the images on video tape will be similar to a concept worked out by W. Hopmann, W. Kohlhaas and D. Rusbuelt of KFA Jülich for a Limiter Surface Temperature Measurement System for JET.

For storage of the video signals a Sony BVU-820 videorecorder with professional image quality will be used. Each single frame of the recording can be coded and identified by a Sony time code generator/reader. The encoding consists of time of the day (hours, minutes, seconds), frame numbering within a second and 8 4-bit words to be defined by the user. These may be used to record the JET discharge number and an additional pellet injector number to identify pellet shots between the JET discharges. The pellet injector number will be generated by a non-volatile counter which is interfaced by 16-bit LSD inputs. The videorecorder and the time coder are equipped with 32-bit parallel interfaces for remote control. These can be connected to 4 CAMAC I/O modules (CPR1) which in turn are controlled by an auxiliary crate controller (CAC). The auxiliary controller will be programmed to

- start recording at the beginning of the JET pulse
- stop recording and memorize the last recorded frame at the end of the JET pulse
- return to the last recorded frame in the parameter setup phase (new recording will be inhibited if this position cannot be reached in time).

The same operations must be executed for pellet test shots without JET discharge. In this case the signals for parameter setup and pulse phase are not generated by the central timing system but internally by the Simatic control system. The timing signals are handled by a CAMAC timer (CTM1).

Between the shots the recording may be reviewed by a TV monitor in the control room (transmitted by the CODAS video network) as a slow-motion or still picture display. The relevant time codes and shot numbers are displayed on the mobile console screen for search and identification purposes.

List of hardware

1 Laser, Laser Diode LT-139

1 Video-camera, English Electric Valve P4300 or Fairchild 3000 (European TV-standard)

1 Power switch (Eurocard, to be developed)

1 Double exposure inhibit (Eurocard, to be developed)

1 Non-volatile pulse counter (Eurocard, to be developed)

1 Video tape recorder Sony BVU-820

1 Time code generator/reader Sony BVG-1000

CAMAC and LSD modules are listed separately.

3.6 Interfaces to CODAS

Figure 31 gives an overview of the CAMAC and LSD components and their connections to the associated control and diagnostic devices. More details about the connected circuits are given in the sections noted in the list.

4. List of drawings and items

Separate drawings handed over to JET.

OOB-1EH-1075	Assembly drawing of centrifuge injector
OB -1EH-1076	Injector arrangement and support structure
3J -1EH-1077	Pellet gas supply
3J -1EH-1078	Centrifuge liquid He supply
2B -1EH-1079	Extrusion cryostat
2B -1EH-1080	Storage cryostat
OC -1EH-1081	Arrangement of feed-in mechanism
2C -1EH-1082	Arrangement of feed-in mechanism
1C -1EH-1056	Rotor for JET pellet injection
1D -1EH-1057	Upper rod suspension
1D -1EH-1065a	Lower rod suspension
3D -1EH-1058a	Centrifugal rod

Items list for drawing No. 00B-1EH-1075 (Fig. 4 and 5)

	material	manufacturerer
1. support frame, AlMgSi 0,5 F22	3.3206.71	
2. adjusting device	1.4311	
3. fitting ring	1.4311	
4. centrifuge vacuum vessel	1.4311	
5. cover flange of centrifuge vessel	1.4311	
6. Helicoflex double sealing		ATW
7. diagnostic window DN150CF	1.4311	Leybold-Heraeus
8. blanking flange DN150CF	1.4311	
9. basic flange for pellet feed in	1.4311	
10. stepping motor f. D_2-rod transport		Berger
11. stepping motor f. pellet cutter		Berger
12. extrusion cryostat		Leybold-Heraeus
13. liquid helium pipe	1.4301	
14. rotor hub, AlZnMgCu 1.5F50	3.4365.71	
15. pellet inlet tube AlMgSi 0.5F13	3.3206.51	
16. rotor rod	CFC	
17. basic flange for rotor drive	1.4311	
18. burst protection ring	1.4311	
19. flange f. pumps DN150 JET RH	1.4311	
20. turbomolecular pump TPU 510A		Pfeiffer
21. a+b flange f. branch pipe unit DN65 RH	1.4311	
22. a+b Branch pipe unit I		
23. fast closing valve DN100		Cetec AG
24. support clamp f. beam line	1.4311	
25. insulator	Hgw 2372, DIN 7735	
26. flange DN 150 RH	1.4311	
27. reducing flange CN 150/100	1.4311	
28. insulating compensator	Al_2O_3/1.4301	Leybold-Heraeus

	material	manufacturer
29. ceramic break	Al_2O_3	
30. flange DN100 CF	1.4311	
31. diagnostic window DN 35 CF		Leybold-Heraeus
32. microwave guide	Cu	
33. microwave vacuum window		
34. pellet exit slit		
35. support frame insulation	Hgw 2372, DIN 7735	
36. centrifuge rotor drive		Beckmann
37. turbomolecular pump TPU 040		
38. pneumatic cylinder		Bosch
39. bellows for adjusting of cryostat	1.4311	
40. all-metal valve DN 250, JET model series 43		VAT
41. flange DN 225 RH	1.4311	
32. reduction flange DN 225/150 RH	1.4311	
43. bellows DN 170, linear extension ± 45 mm	1.4311	

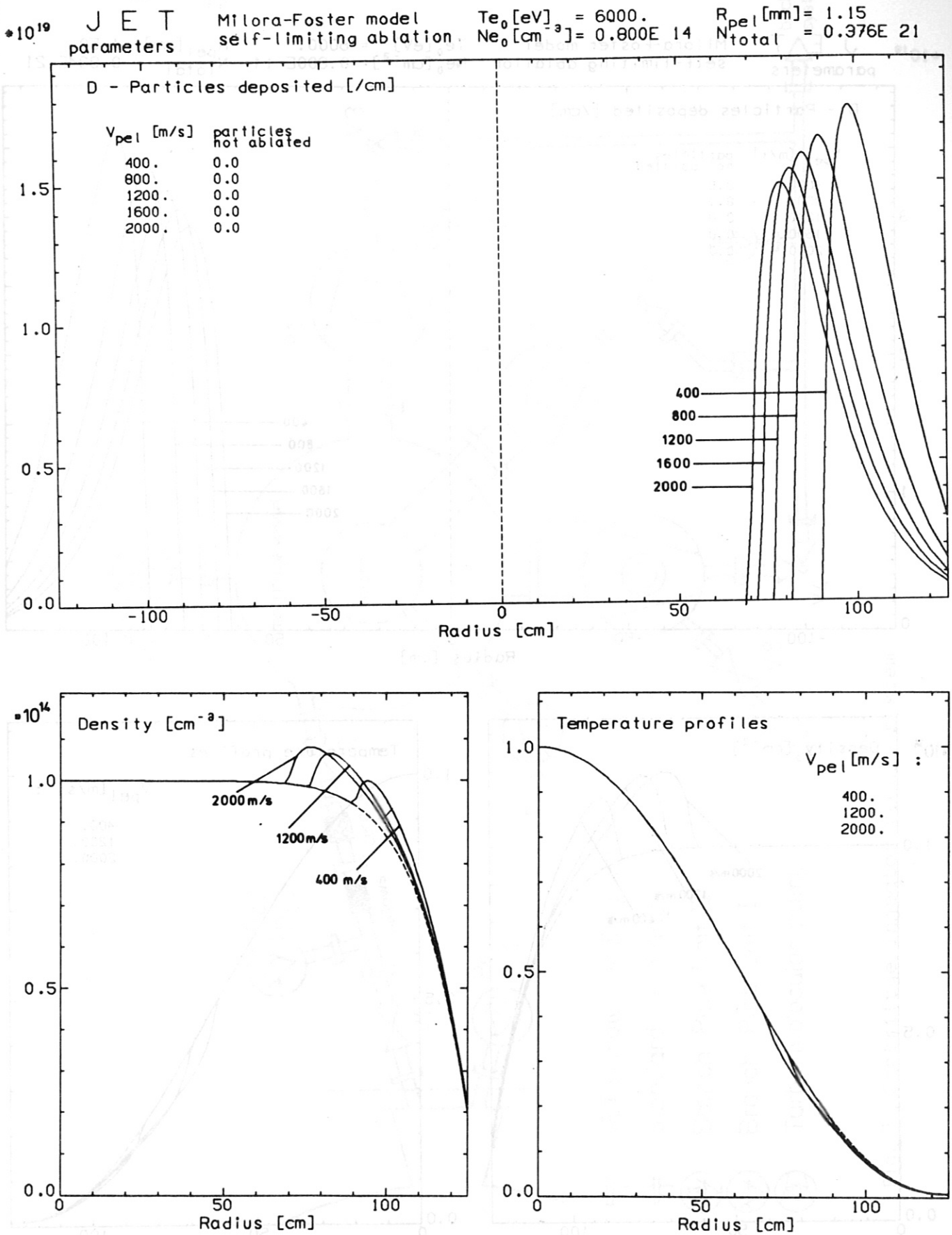

Fig. 1 Particle deposition, density and temperature profile for pellet size d = 2.3 mm

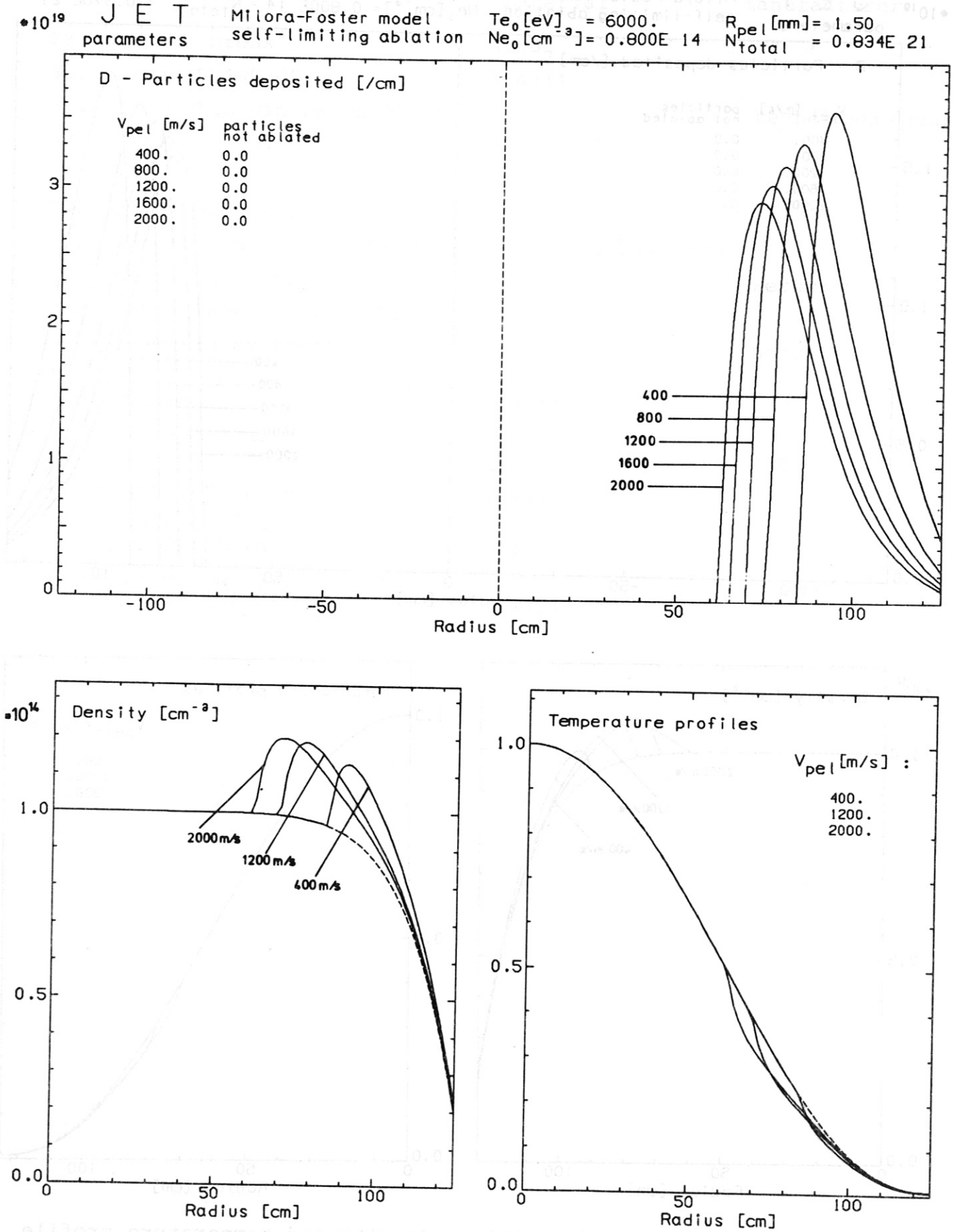

Fig. 2 Particle deposition, density and temperature profile for pellet size d = 3.0 mm

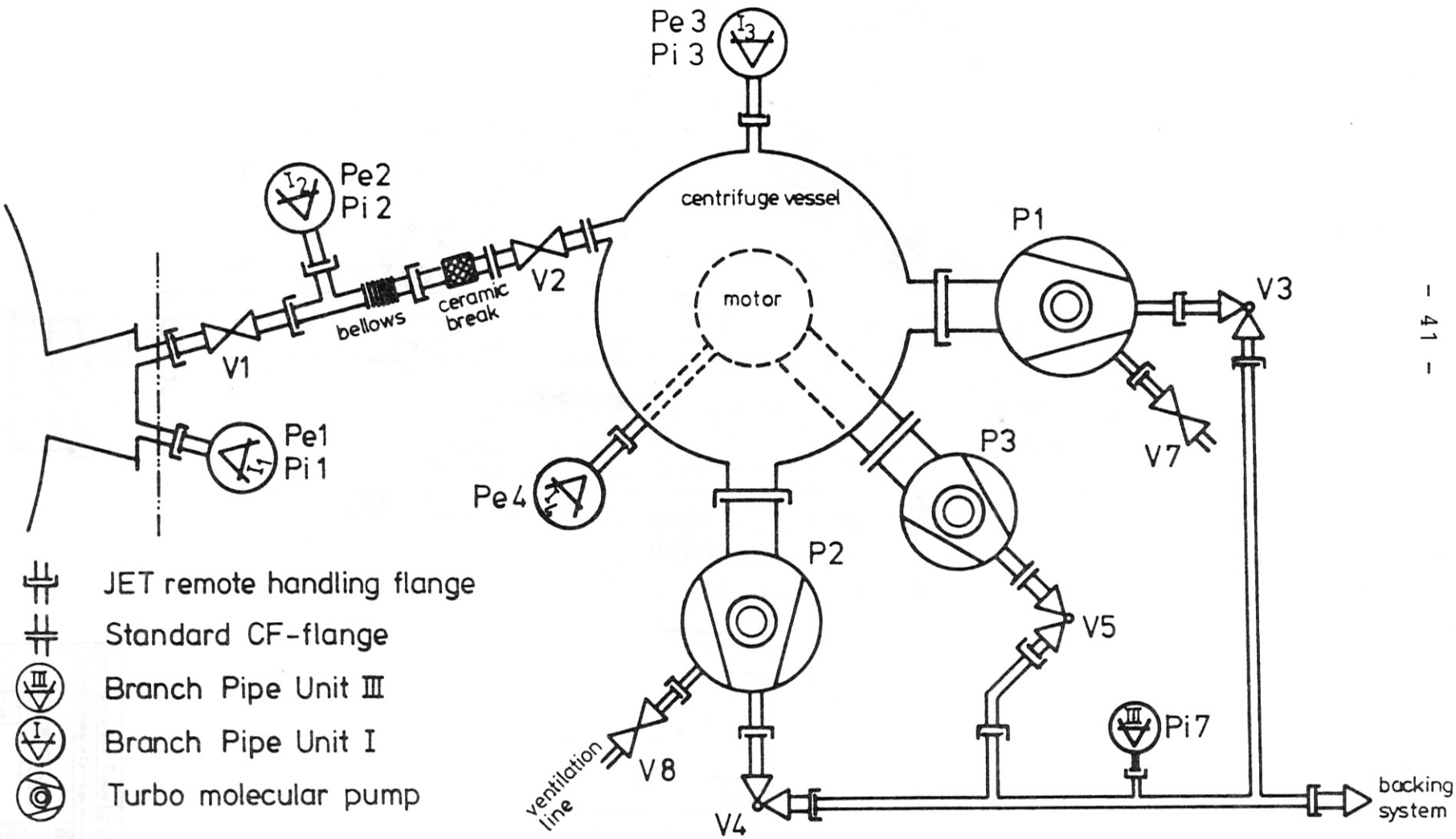

Fig. 3 Centrifuge injector vacuum system

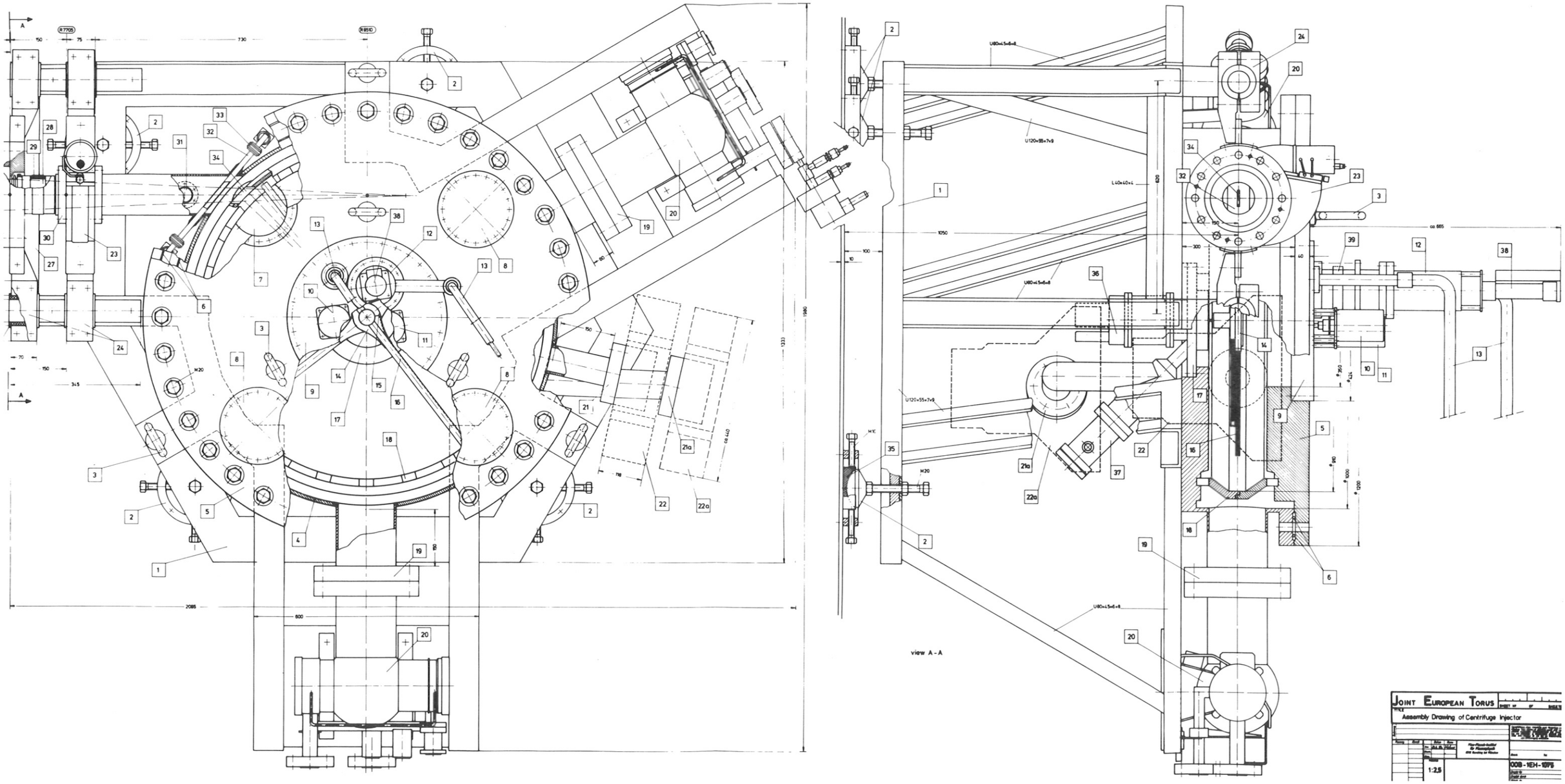

Fig. 4 Assembly drawing of centrifuge injector

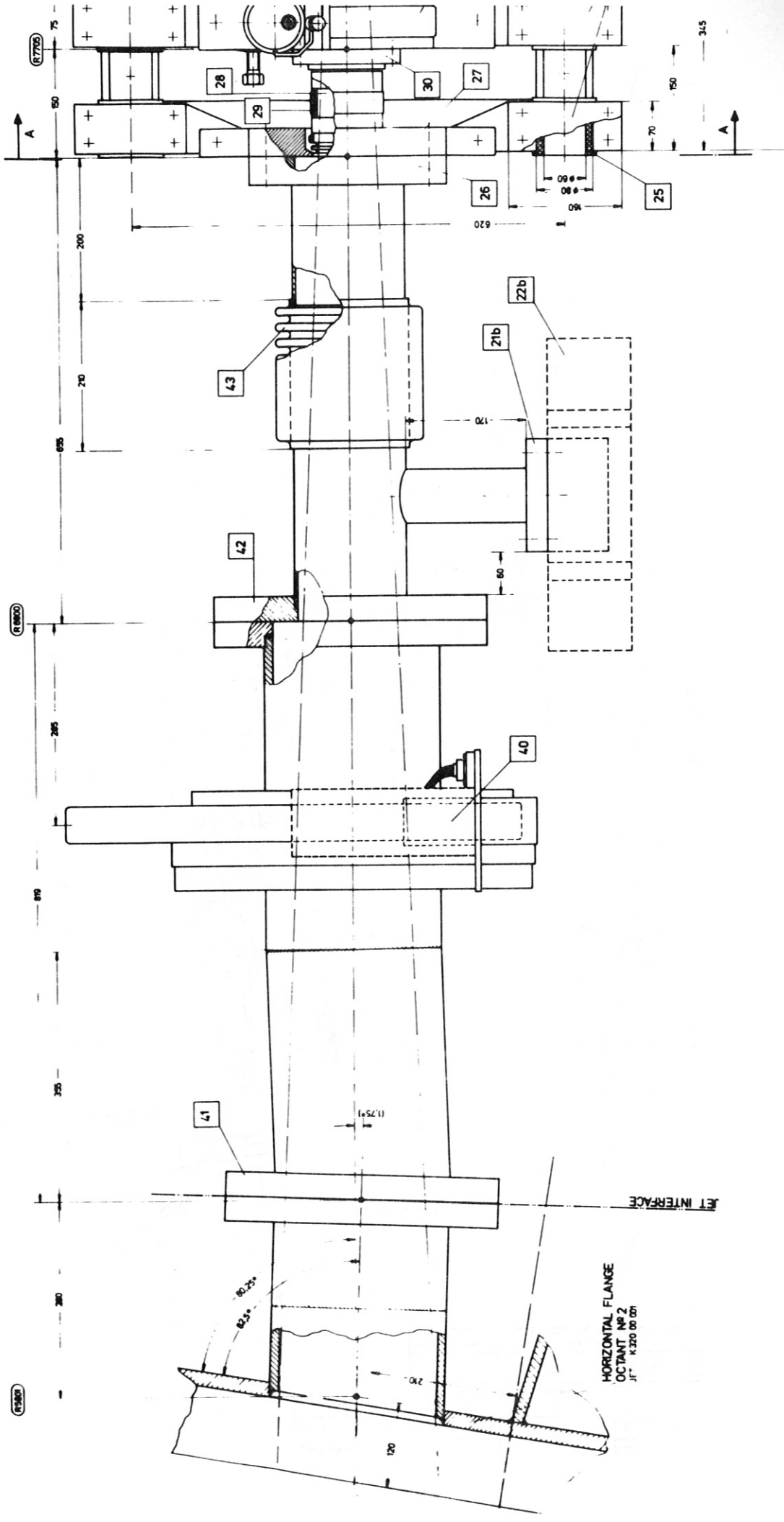

Fig. 5 Vacuum interface with torus vacuum

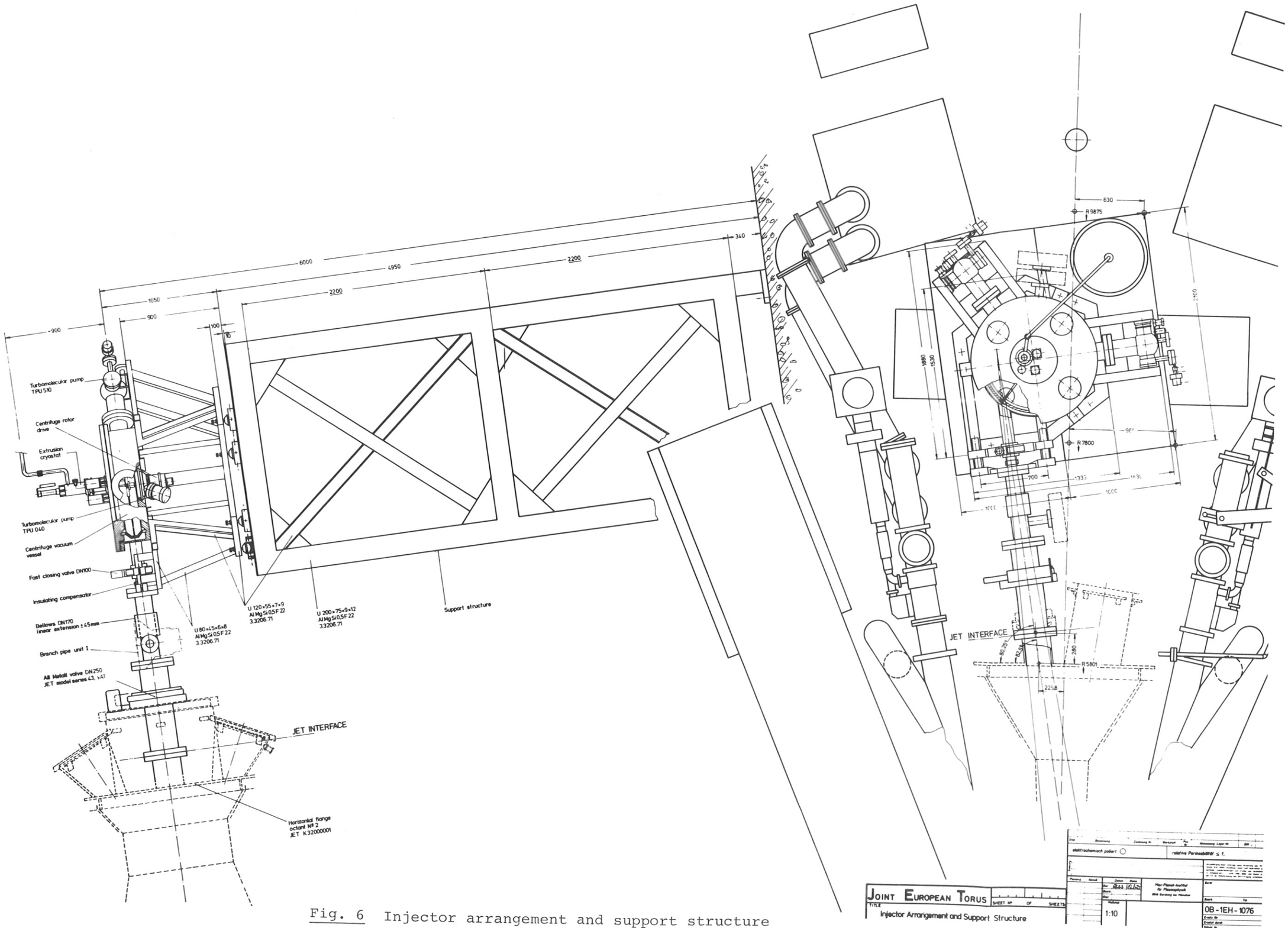

Fig. 6 Injector arrangement and support structure

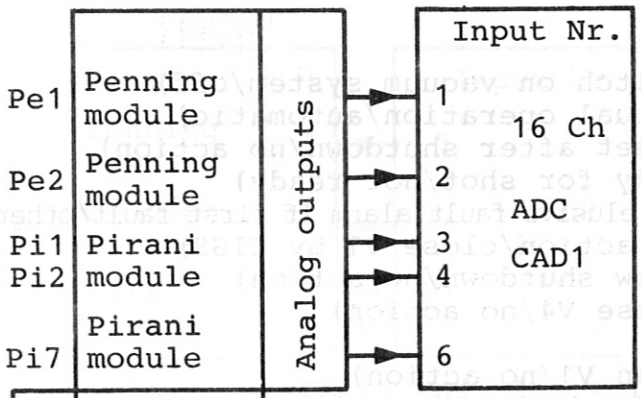

J/O module

Relais	1	LSD In1 (open V1 by CODAS/no action)
Output	2	LSD In2 (close V1 by CODAS/no action)
EA	3	Siematic (open/close V2, if control by EA)
Unit 1	4	Siematic (control of V2 by Siematic/EA)
Ch.Nr.	5	
	6	Power switch V7 (close V7/open)
	7	Power switch V8 (close V8/open)
	8	

Opto	1	LSD out 1 (V1 closed/opened)
Input	2	Feedback switch V2 (V2 closed/opened)
EA	3	
Unit 2	4	Feedback switch V7 (V7 opened/closed)
Ch.Nr.	5	Feedback switch V8 (V8 opened/closed)
	6	
	7	
	8	Feedback switch cooling water P1 (P1 on/off)

J/O module

Relais	1	
Output	2	Power switch cooling water (on/off)
EA	3	LSD In 3 (cooling water P1 elusive fault alarm
Unit 3	4	LSD In 4 (cooling water P2 if first fault detected
Ch.Nr.	5	LSD In 5 (cooling water P3/otherwise
	6	
	7	LSD In 7 (vacuum system on/off)
	8	LSD In 8 (manual operation/automatic)

Opto	1	Feedback switch cooling water P2 (P2 on/off)
Input	2	Feedback switch cooling water P3 (P3 on/off)
EA	3	
Unit 4	4	LSD Out 2 (reset after shutdown/no action) pulsed
Ch.Nr.	5	EB U1 Ch1 (Pe3-4 low/either of Pe3-4 high)
	6	LSD Out 3 (switch on vacuum system/off)
	7	LSD Out 4 (manual operation/automatic)
	8	

Fig. 7 /1 Vacuum control system

J/0 module	Relais Output EA Unit 5 Ch.Nr.	1 2 3 4 5 6 7 8	EB U2 Ch1 (switch on vacuum system/off) EB U2 Ch2 (manual operation/automatic) EB U2 Ch3 (reset after shutdown/no action) LSD In 9 (ready for shot/not ready) LSD in 10 (Pi7 elusive fault alarm if first fault/otherwise) LSD In 11 (no action/close V1 by CISS) LSD In 12 (slow shutdown/no action) EB U6 Ch7 (close V4/no action)
	Opto Input EA Unit 6 Ch.Nr.	1 2 3 4 5 6 7 8	LSD Out 5 (open V1/no action) LSD Out 6 (close V1/no action) EB U3 Ch4 (slow shutdown/no action)
J/0 module	Relais Output EA Unit Ch.Nr.	1 2 3 4 5 6 7 8	
	Opto Input EA Unit Ch.Nr.	1 2 3 4 5 6 7 8	

Feedback switch V1 - LSD In 13 (on/off)
" V7 - LSD In 15 (on/off)
" V8 - LSD In 16 (on/off)
Feedback switch cooling water P1 - LSD In 19 (on/off)
" P2 - LSD In 20 (on/off)
" P3 - LSD In 21 (on/off)

Fig. 7 /2 Vacuum control system

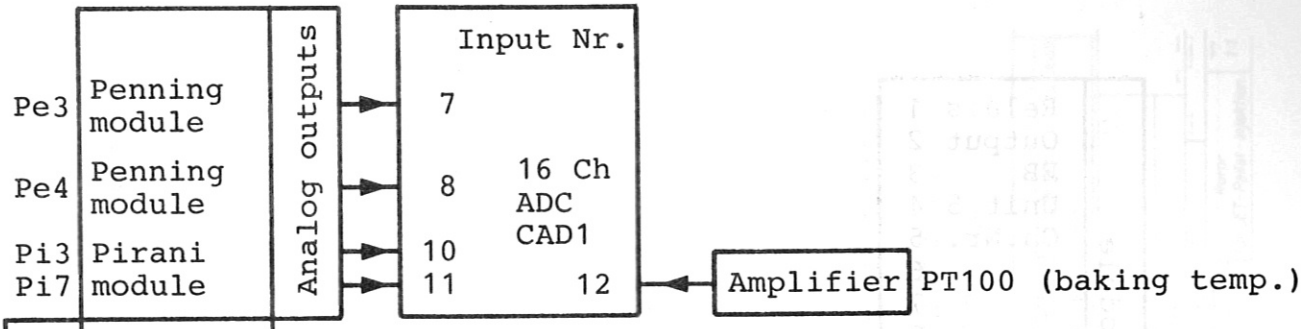

J/O module

Relais	1	EA U4 Ch5 (Pe3-4 low/either of P3-4 high)
Output	2	Power switch V3 (open V3/close)
EB	3	Power switch V4 (open V4/close)
Unit 1	4	Power switch V5 (open V5/close)
Ch.Nr.	5	Power switch P1 (P1 on/off)
	6	Power switch P2 (P2 on/off)
	7	Power switch P3 (P3 on/off)
	8	Siematic (Pi3 high/low)

Opto	1	EA U5 Ch1 (switch on vacuum system/off)
Input	2	EA U5 Ch2 (manual operation/automatic)
EB	3	EA U5 Ch3 (reset after shutdown/no action)
Unit 2	4	Feedback switch V3 (V3 closed/opened)
Ch.Nr.	5	Feedback switch V4 (V4 closed/opened)
	6	Feedback switch V5 (V5 closed/opened)
	7	Feedback switch P1 (P1 on/off)
	8	Feedback switch P2 (P2 on/off)

J/O module

Relais	1	LSD In 23) (P1 elusive fault alarm
Output	2	LSD In 24) (P2 if first fault detected
EB	3	LSD In 25) (P3/otherwise
Unit 3	4	EA U6 Ch3 (slow shutdown/no action)
Ch.Nr.	5	
	6	
	7	
	8	

Opto	1	Feedback switch P3
Input	2	LSD Out 7 (manual V3 open/no action)
EB	3	LSD Out 8 (manual V3 close/no action)
Unit 4	4	LSD Out 9 (manual V4 open/no action)
Ch.Nr.	5	LSD Out 10 (manual V4 close/no action)
	6	LSD Out 11 (manual V5 open/no action)
	7	LSD Out 12 (manual V5 close/no action)
	8	LSD Out 13 (manual P1 on/no action)

Fig. 7/3 Vacuum control system

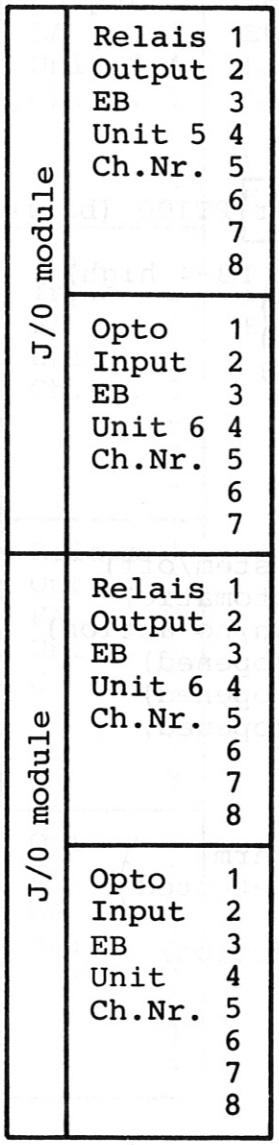

LSD Out 14 (manual P1 off/no action)
LSD Out 15 (manual P2 on/no action)
LSD Out 16 (manual P2 off/no action)
LSD Out 17 (manual P3 on/no action)
LSD Out 18 (manual P3 off/no action)
Siematic (cryostat warm/cold)

Feedback switch V3 - LSD In 26
" V4 - LSD In 27
" V5 - LSD In 28
" P1 - LSD In 29
" P2 - LSD In 30
" P3 - LSD In 31

Fig. 7 /4 Vacuum control system

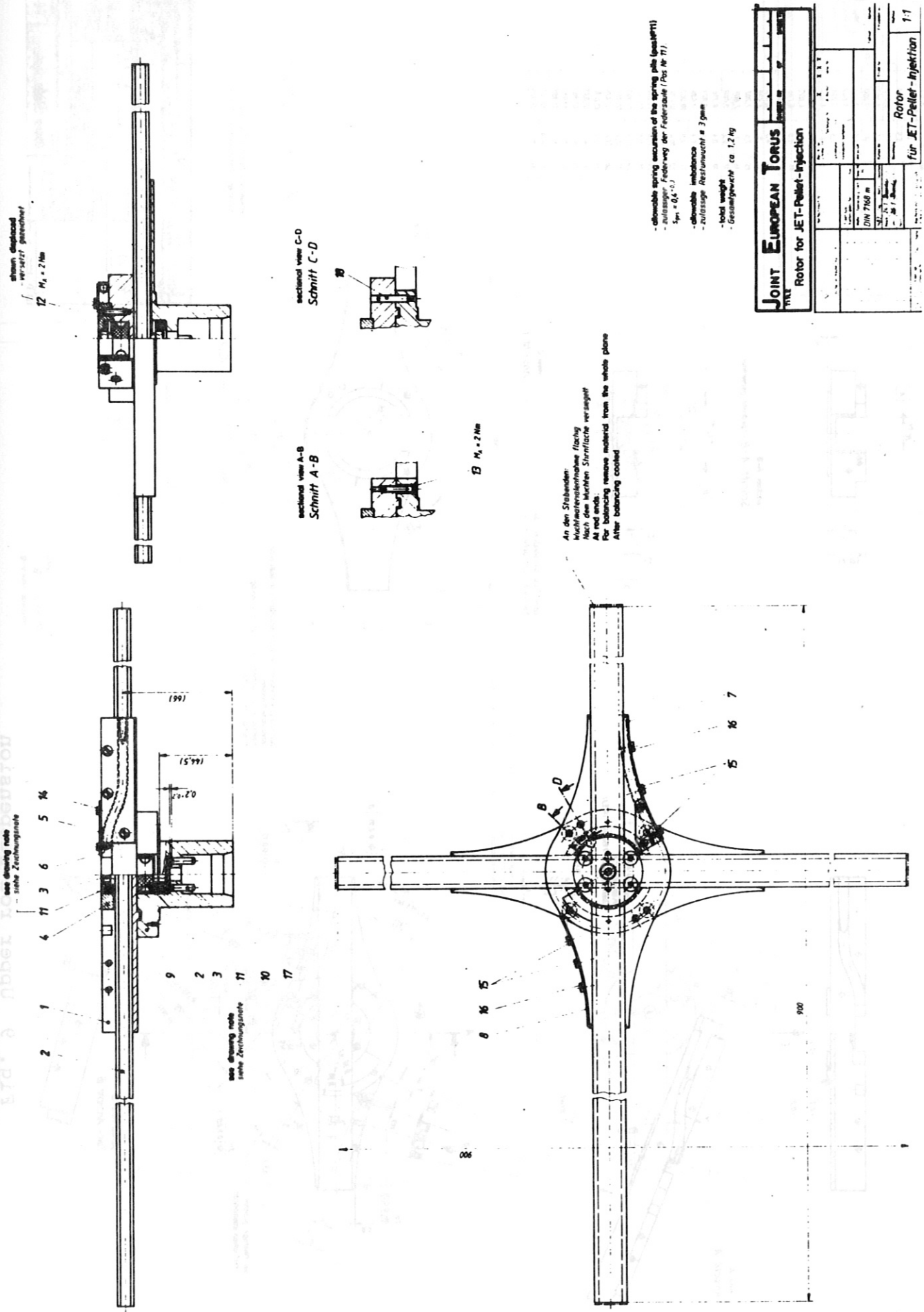

Fig. 8 Assembly drawing of centrifuge rotor

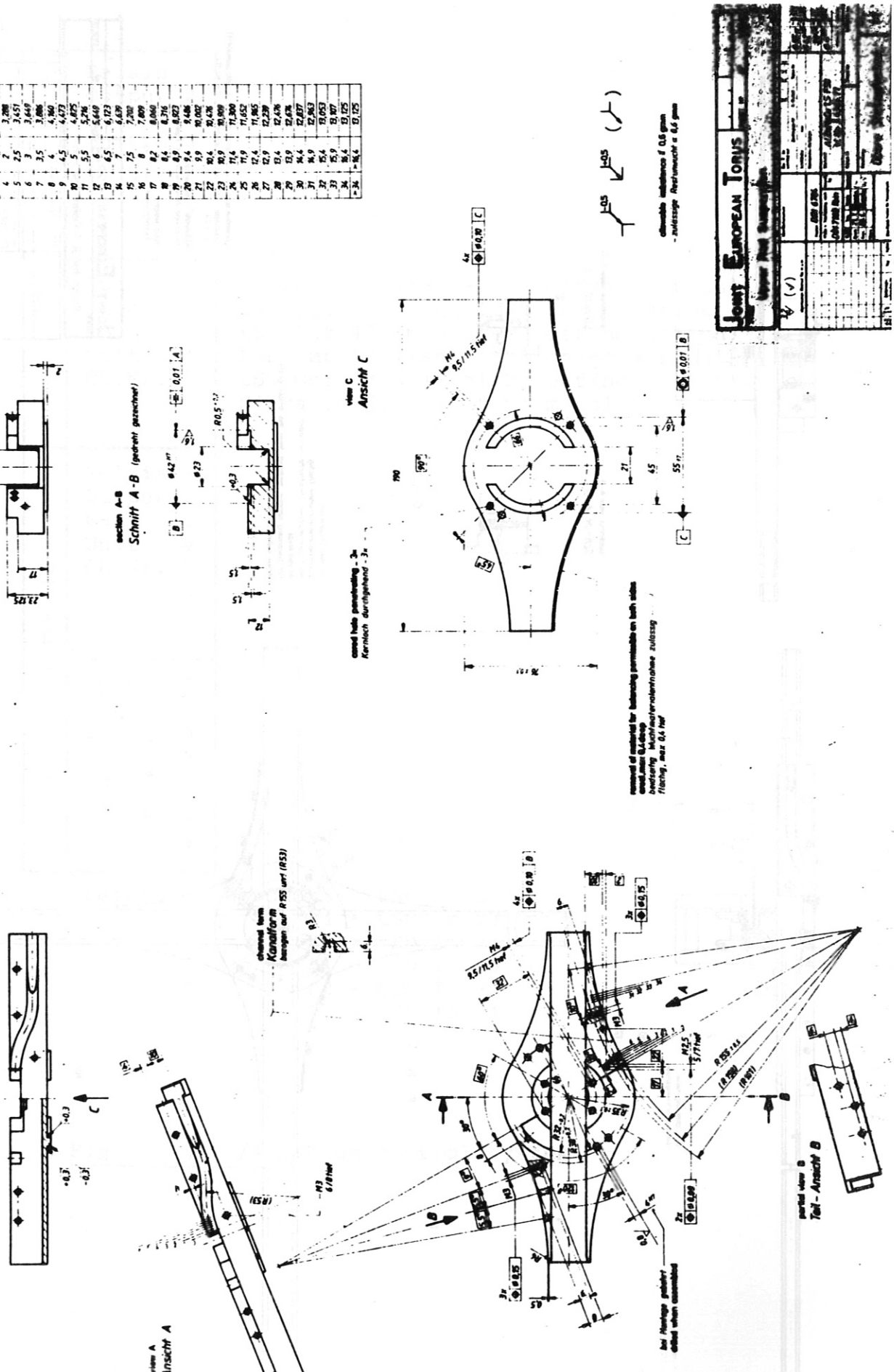

Fig. 9 Upper rod suspension

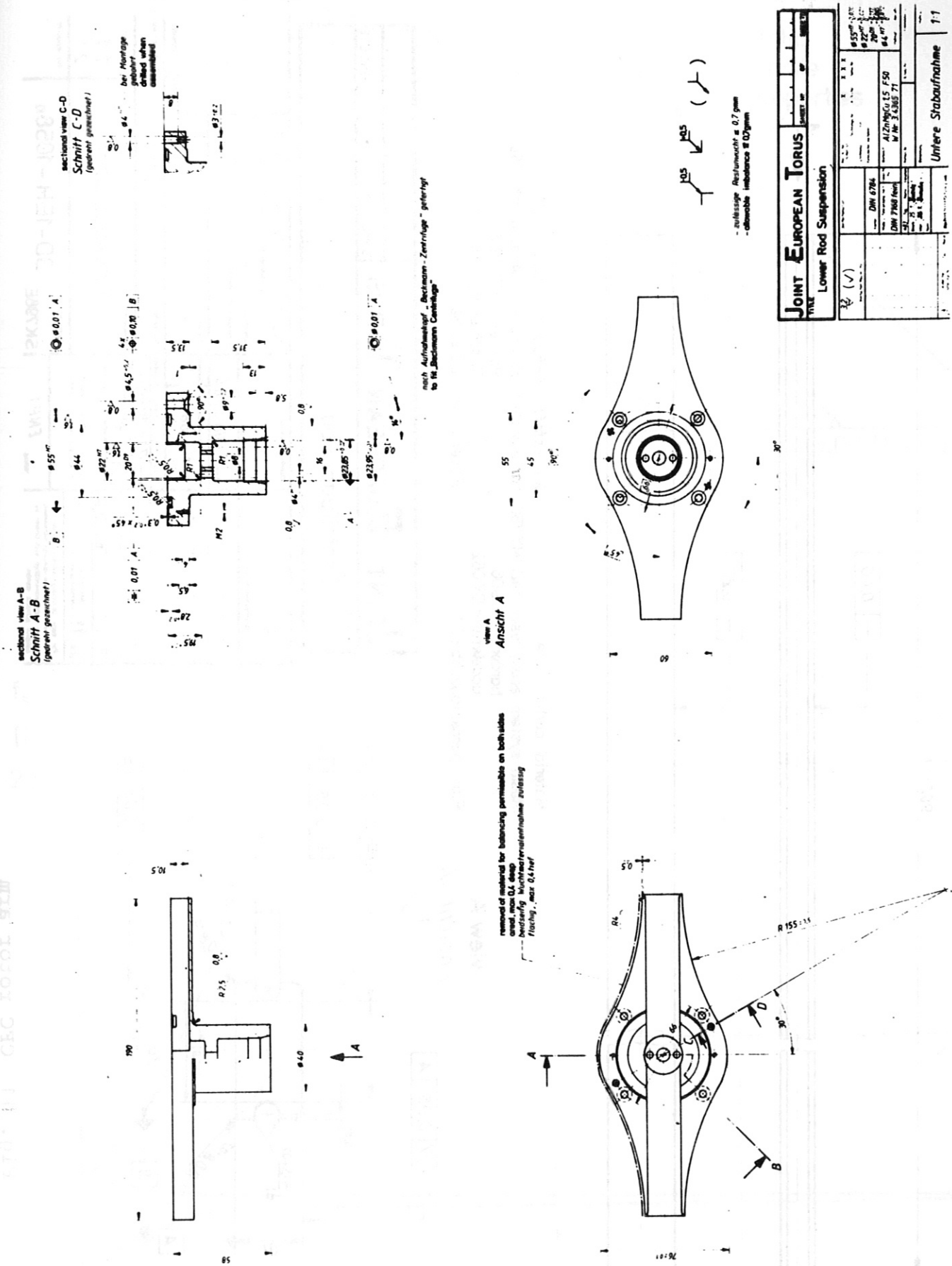

Fig. 10 Lower rod suspension

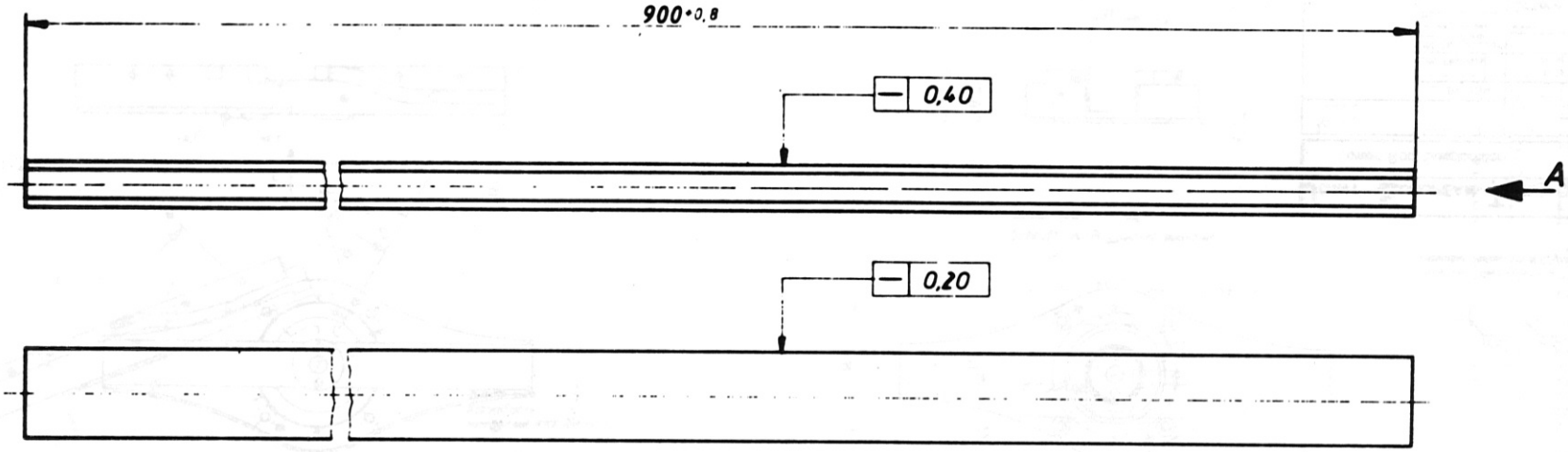

Material: carbon fibre
Resin system: epoxy resin Araldit MY 750
hardener HY 906
accelerator DY 062
Fiber percentage: 65±3%

Werkstoff : C-Faser Torayca T400
Harzsystem : Epoxidharz Araldit MY 750
Härter HY 906
Beschleuniger DY 062
Fasergehalt 65±3%

view A
Ansicht A
2:1

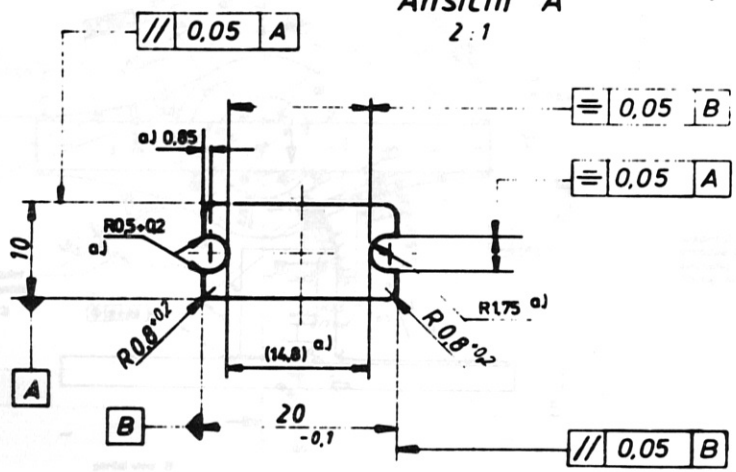

JOINT EUROPEAN TORUS	SHEET Nº	OF	SHEETS
TITLE: Centrifugal Rod			

Oberflächenschutz
Kanten DIN 6784
Maße o. Toleranzang. nach DIN 7168 m
Gewicht kg
Werkstoff
Rohteil-Nr
Ersatz für
Ersetzt durch
Benennung: Schleuderstab
Maßstab 1:1 2:1
Zeichnungs-Nr SK798E 3D-1EH-1058a
Arb.-paket Nr
ENP1

Fig. 11 CFC rotor arm

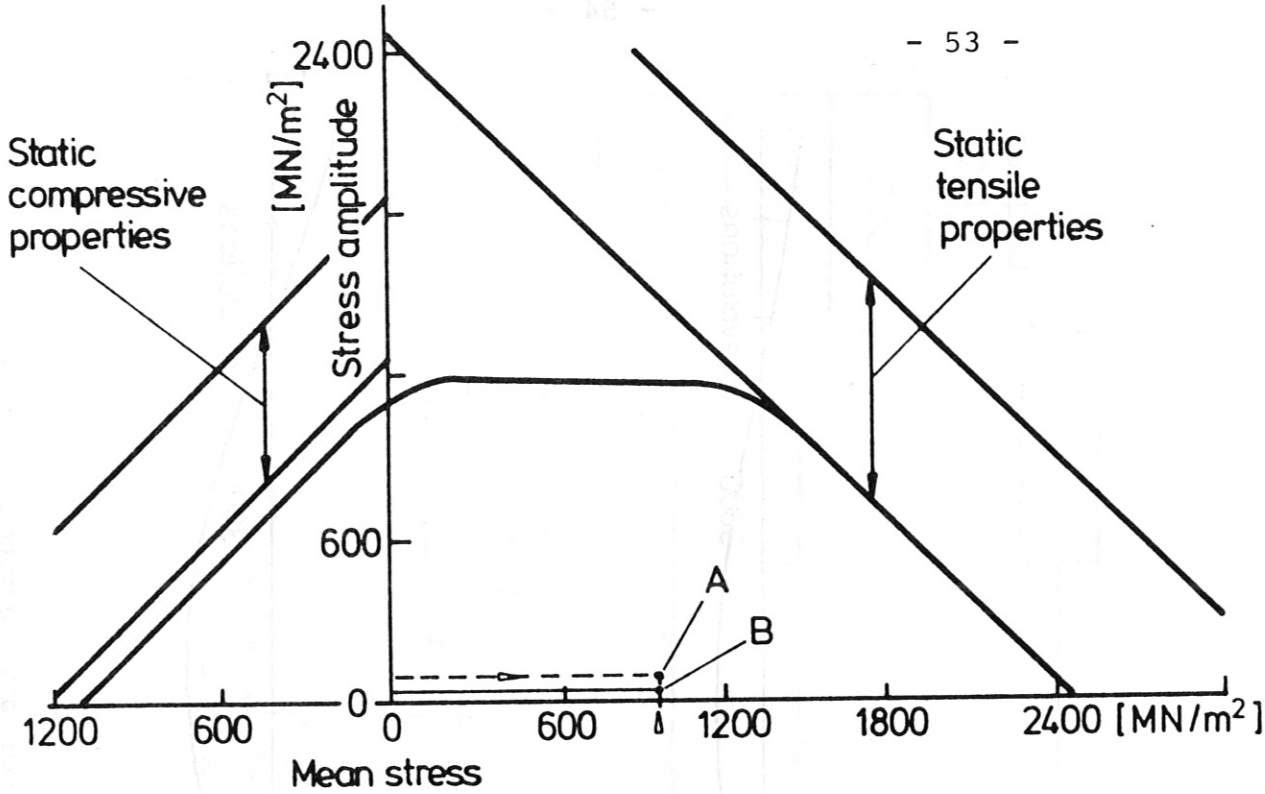

Fig. 12 Life characteristic of the CFC rotor arm for 10^7 load cycles

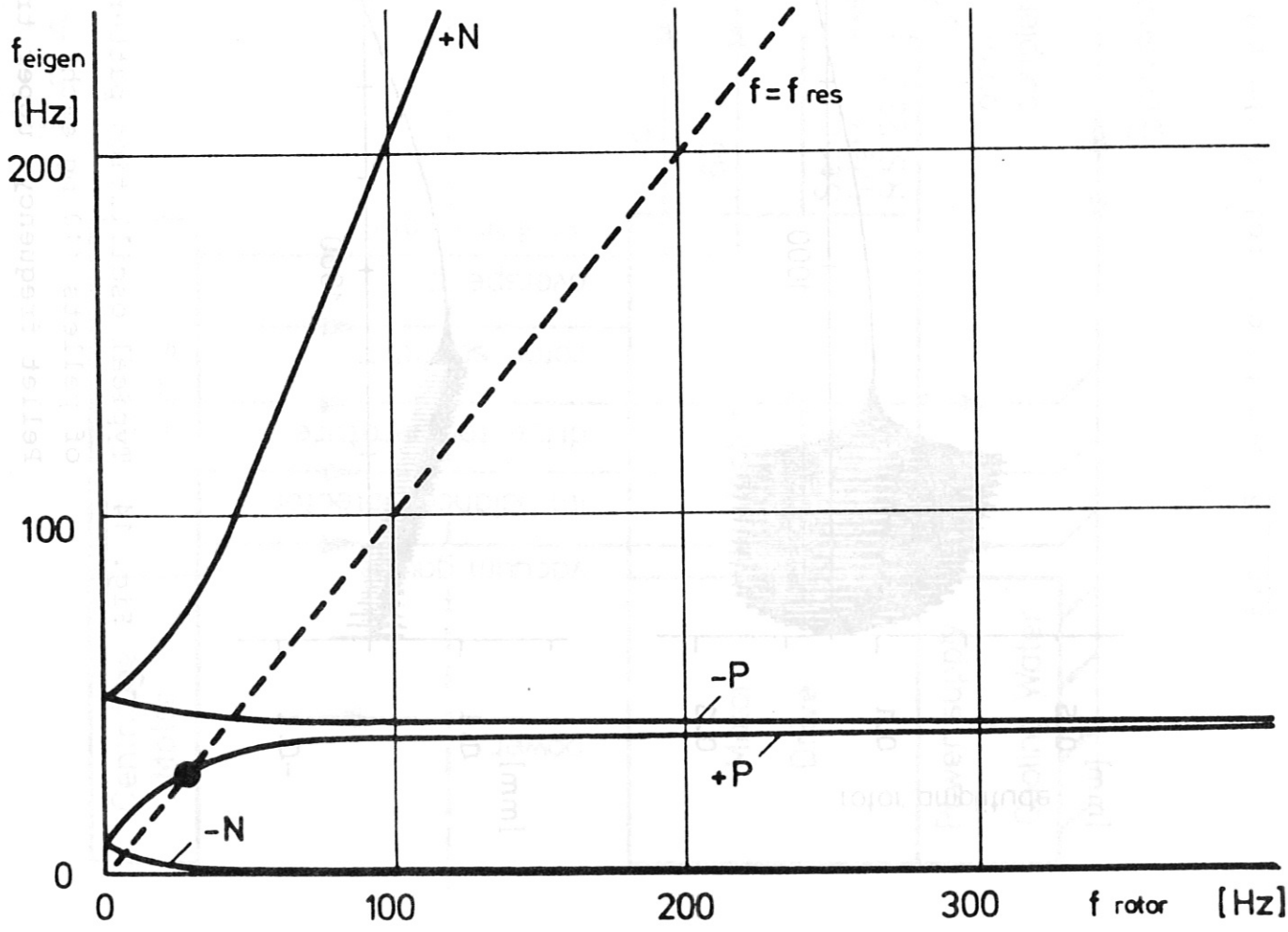

Fig. 13 Eigenvalue of CFC rotor arm depending on revolution frequency

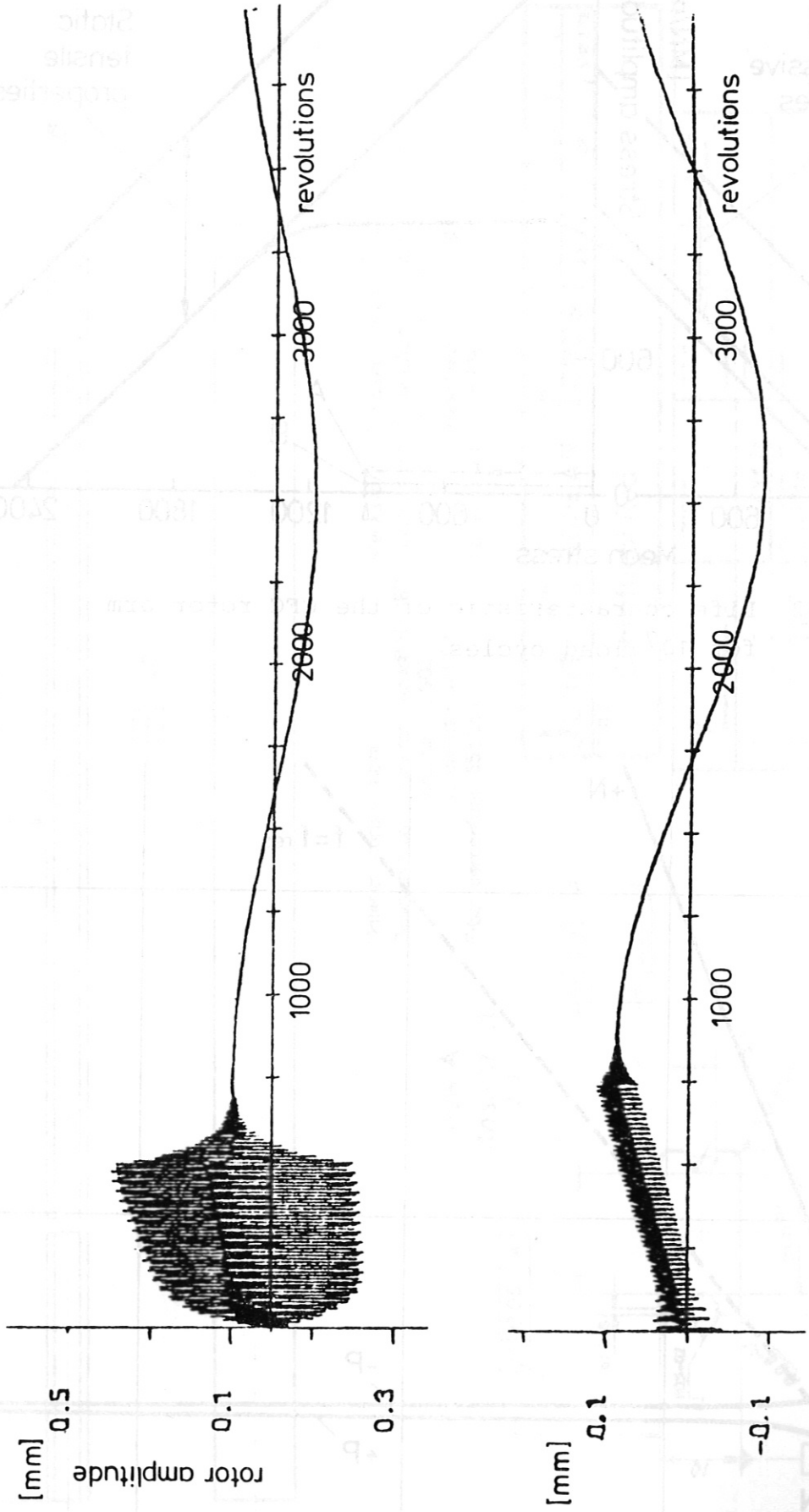

Fig. 14 Typical oscillation pattern of the rotor arm excited by a series of pellets (10 mg each).
Pellet frequency: upper trace 40 Hz, lower trace 27 Hz

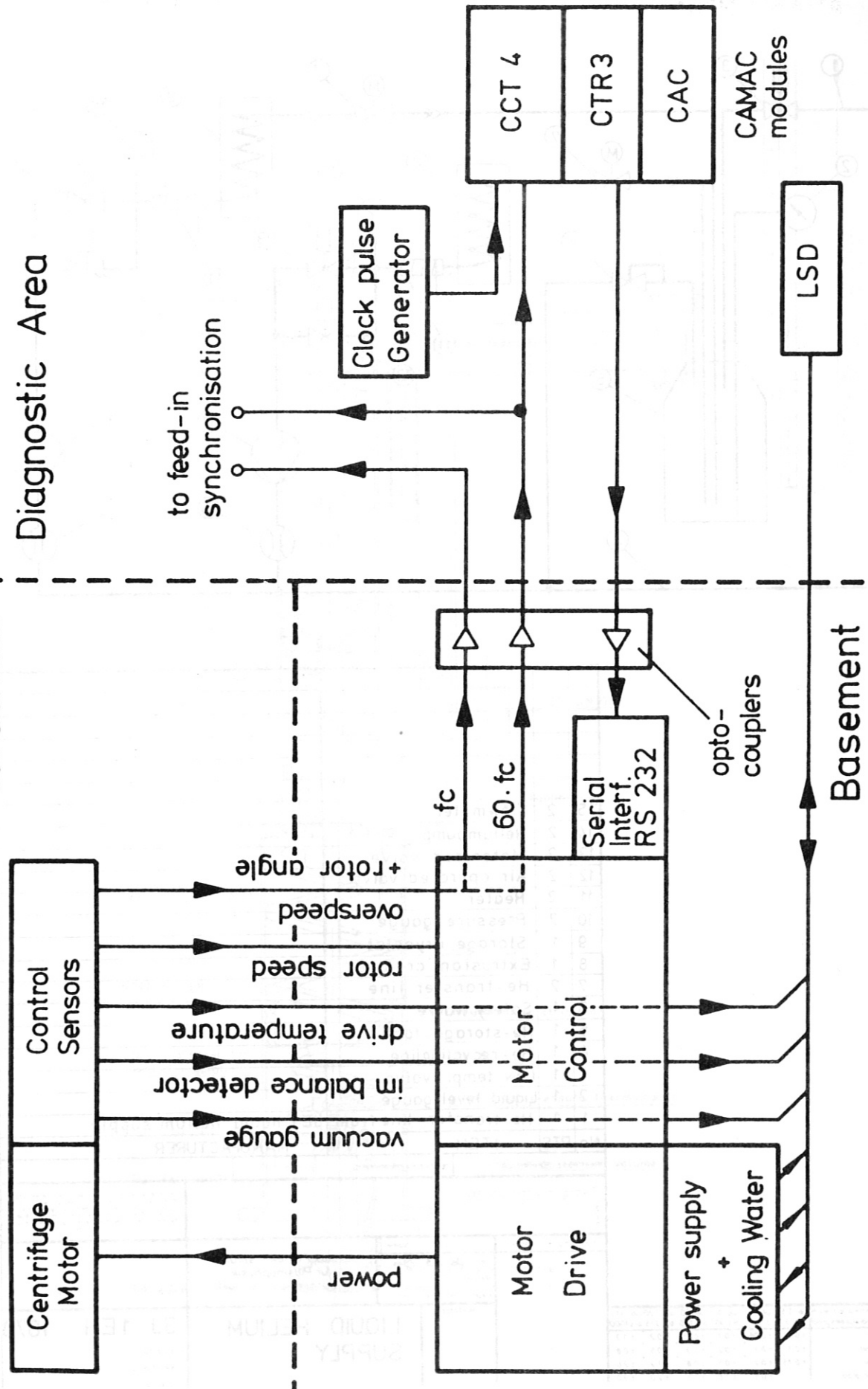

Fig. 15 Remote control of the rotor drive

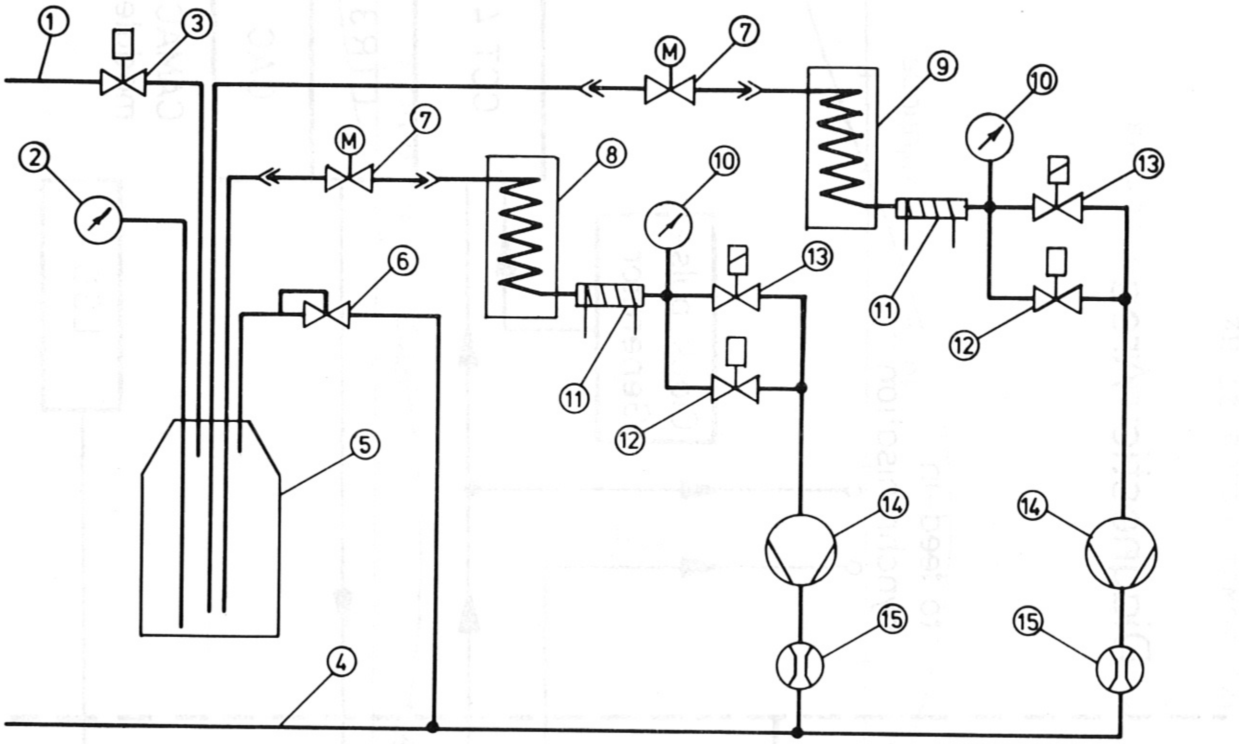

No.	PTS	ITEM	MANUFACTURER
15	2	Flowmeter	
14	2	Heliumpump	
13	2	Motorized valve	
12	2	Air operated valve	
11	2	Heater	
10	2	Pressure gauge	
9	1	Storage cryostat	
8	1	Extrusion cryostat	
7	2	He-transfer line	
6	1	Safety valve	
5	1	He-storage tank	
4	1	He-recyclingline	
3	1	Low temp. valve	
2	1	Liquid level gauge	
1	1	He-transfer line from	JET liquid helium supply

elektrolytisch poliert ○ relative Permeabilität ≤ 1

Änderung

Passung	Abmaß		Datum	Name		
		Gez	06. 83	Bu	Max-Planck-Institut für Plasmaphysik 8046 Garching bei München	Bearb Te
		Bearb				
		Gepr				
		Maßstab			LIQUID HELIUM SUPPLY	3J 1EH 1078 Ersatz für Ersetzt durch Druck Nr

Nennmaßbereich / Genauigkeitsgrad	üb 0,5 bis 3	üb 3 bis 6	üb 6 bis 30	üb 30 bis 120	üb 120 bis 315	üb 315 bis 1000
fein	±0,05	±0,05	±0,1	±0,15	±0,2	±0,3
mittel	±0,1	±0,1	±0,2	±0,3	±0,5	±0,8
grob	±0,15	±0,2	±0,5	±0,8	±1,2	±2,0
sehr grob		±0,5	±1,0	±1,5	±2,0	±3,0

Fig. 16 Scheme of cryogenic system

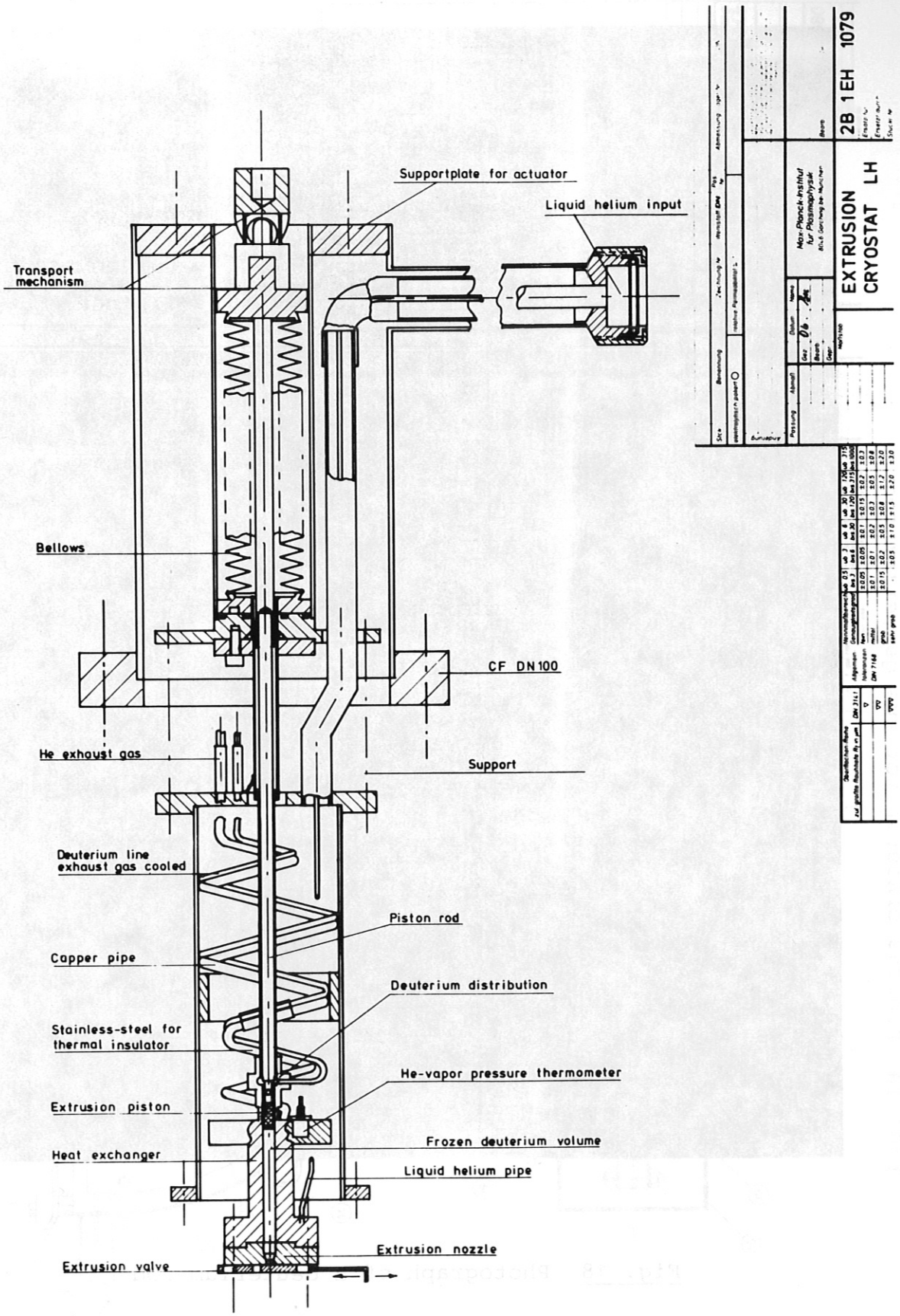

Fig. 17 Leybold-Heraeus extrusion cryostat

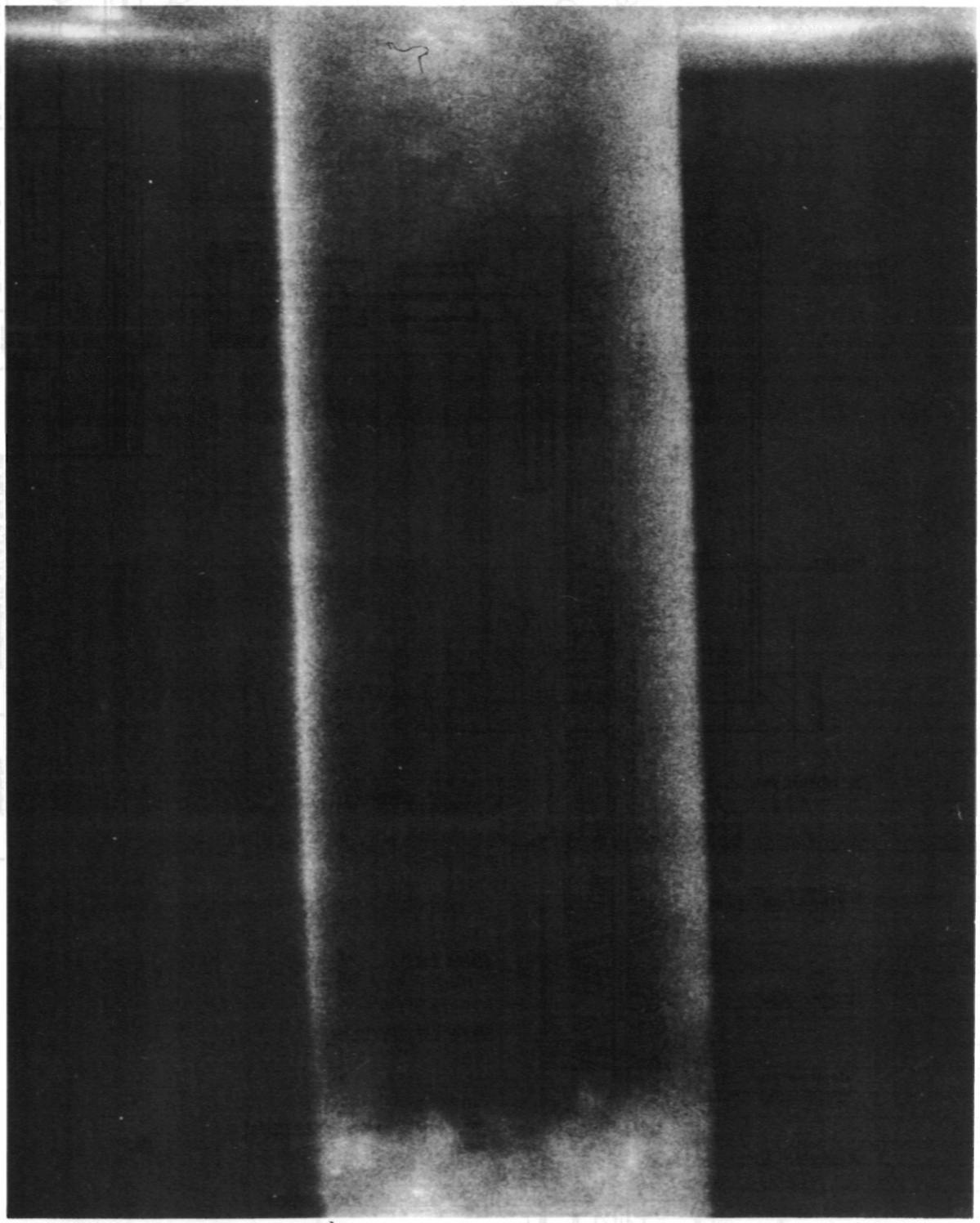

Fig. 18 Photograph of a deuterium rod

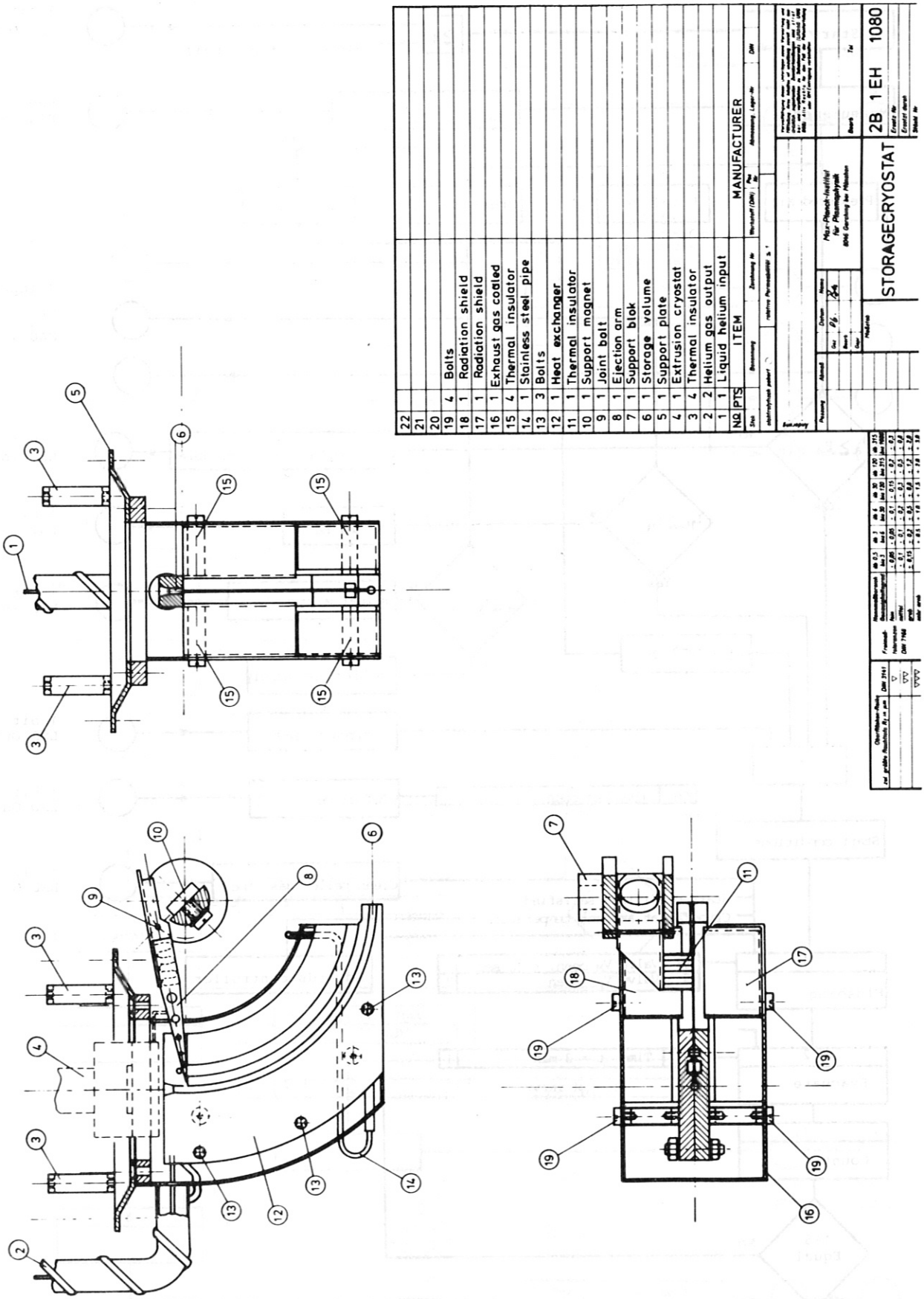

Fig. 19 Storage cryostat for the deuterium rod

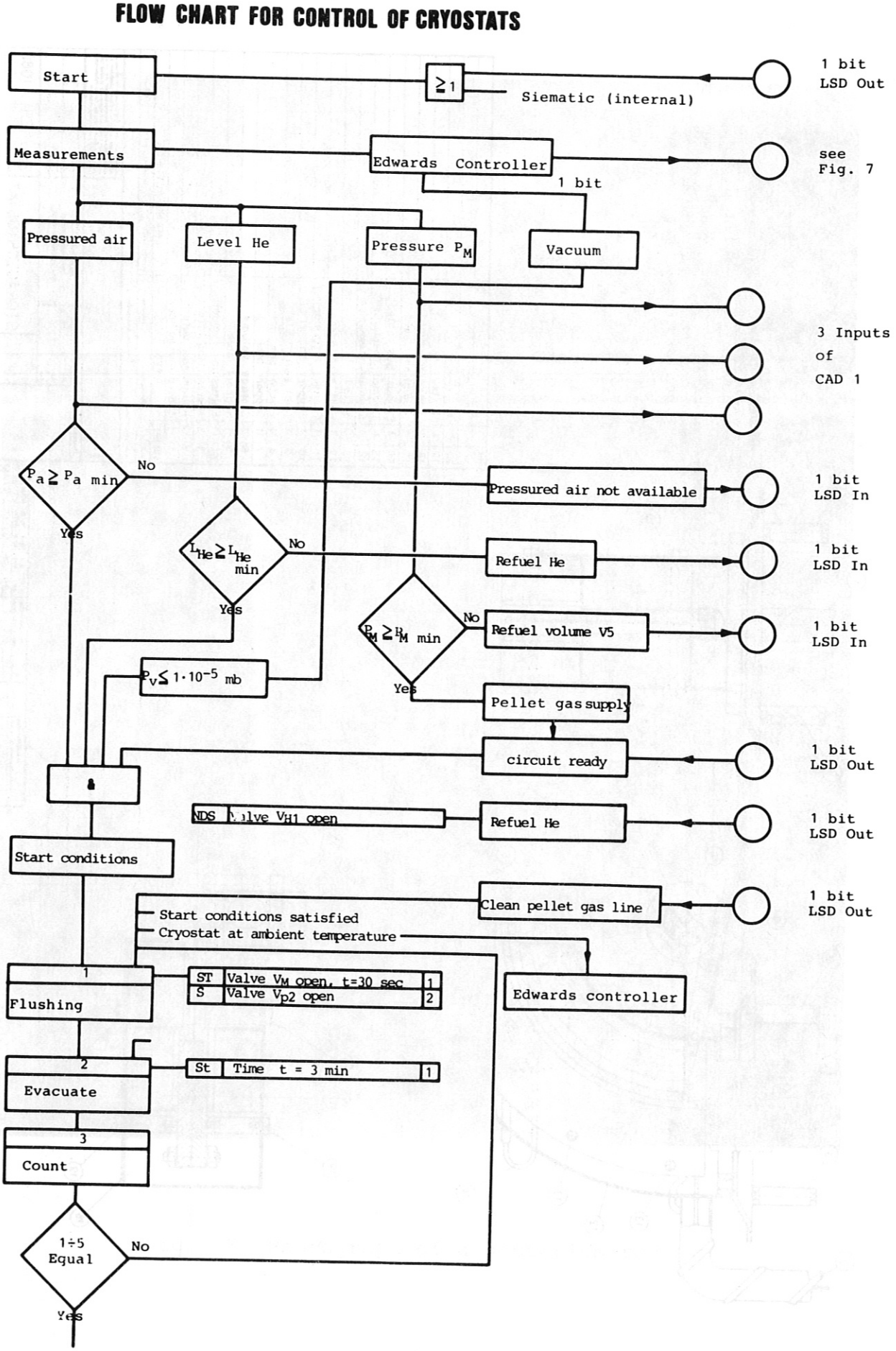

Fig. 20/1 Flow chart for control of cryostats

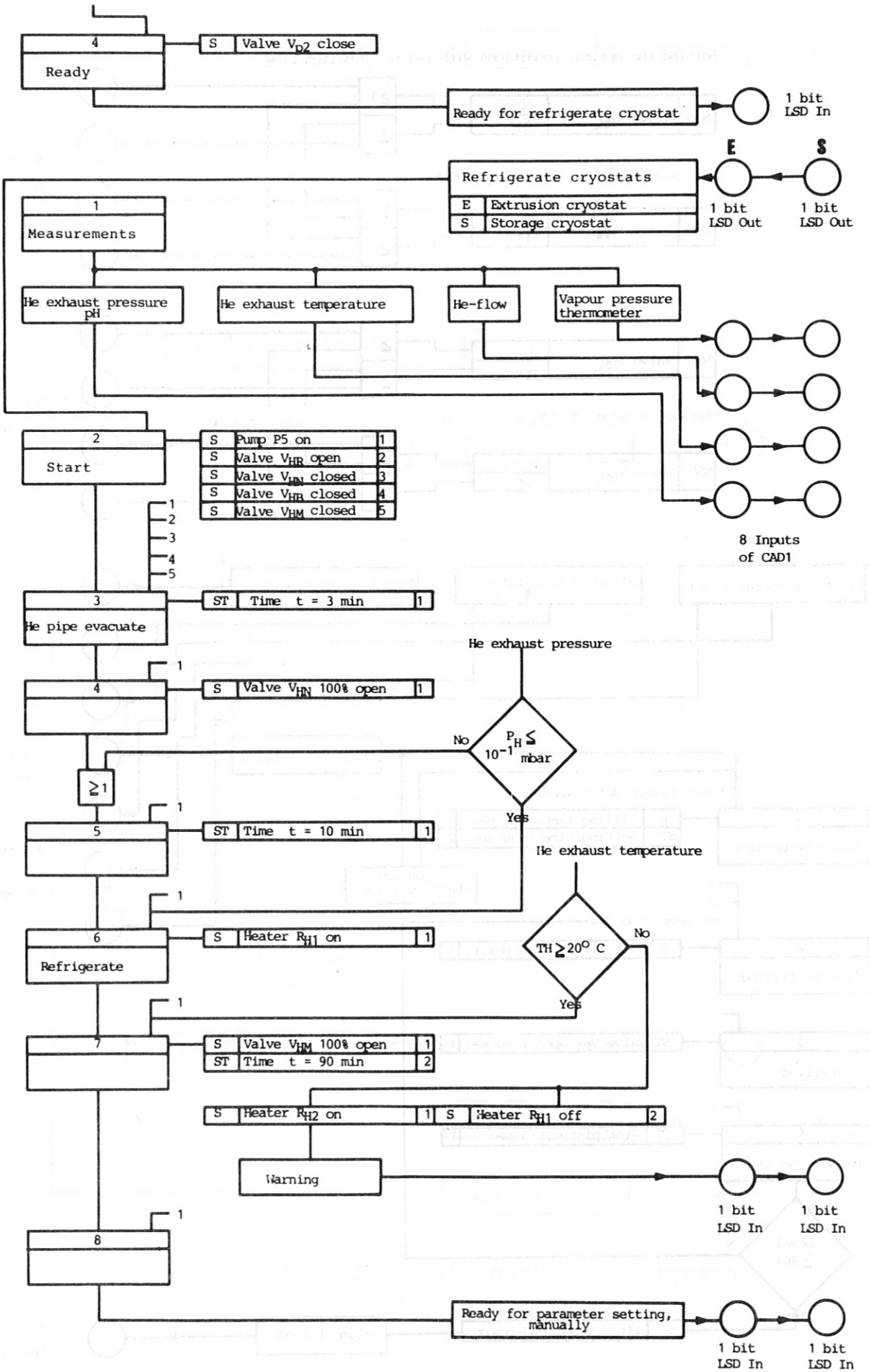

Fig. 20/2 Flow chart for control of cryostats

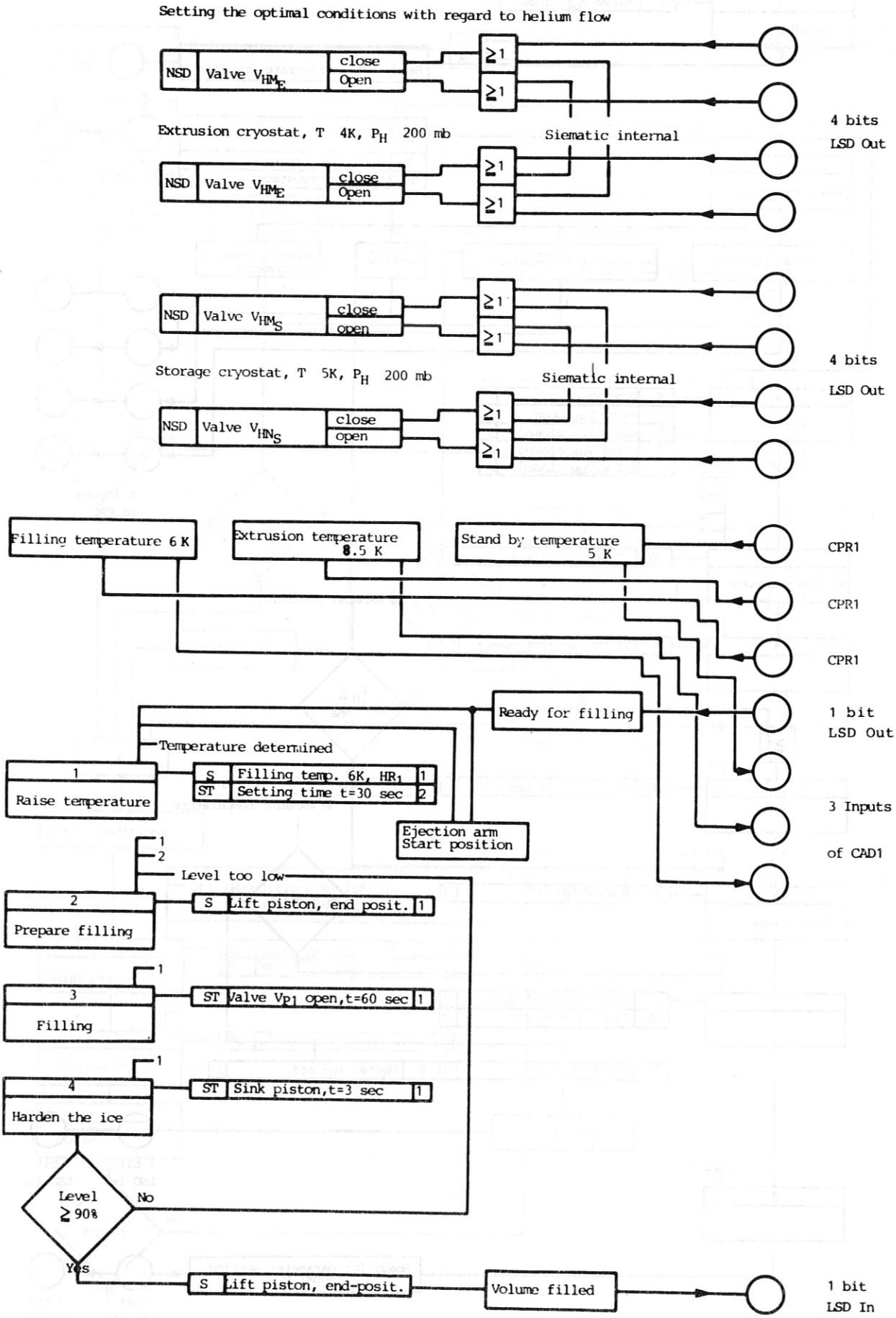

Fig. 20/3 Flow chart for control of cryostats

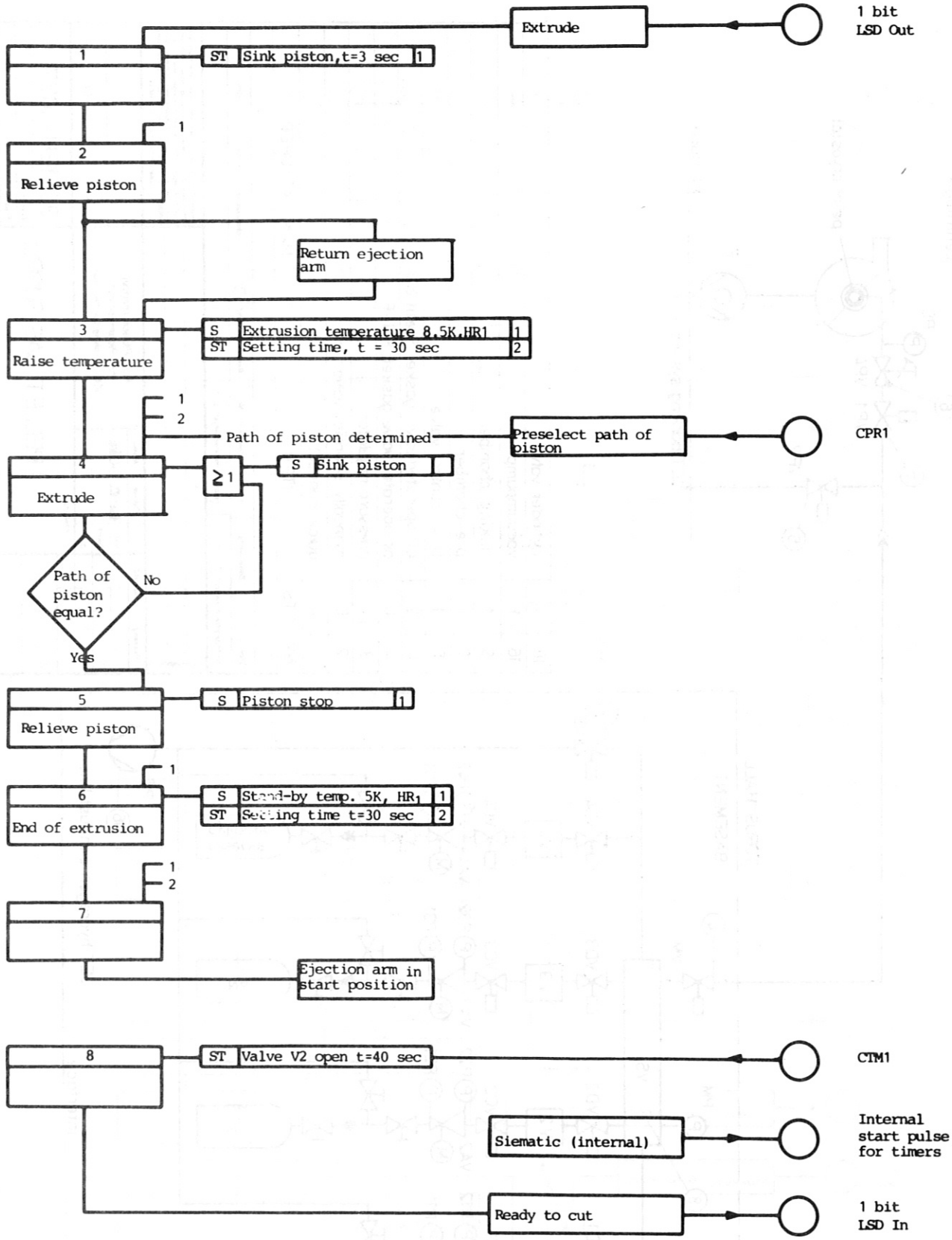

Fig. 20/4 Flow chart for control of cryostats

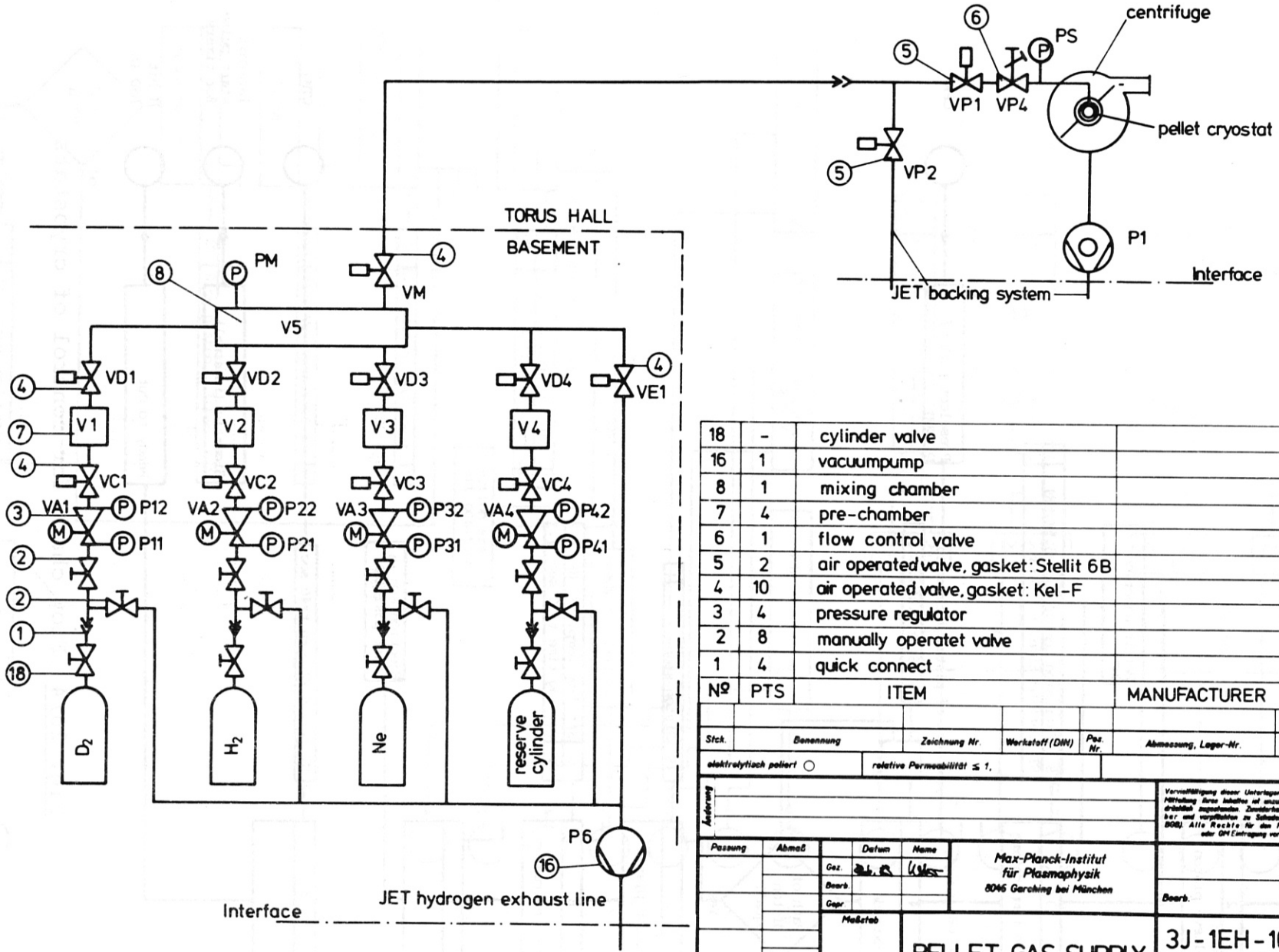

18	-	cylinder valve	
16	1	vacuumpump	
8	1	mixing chamber	
7	4	pre-chamber	
6	1	flow control valve	
5	2	air operated valve, gasket: Stellit 6B	
4	10	air operated valve, gasket: Kel-F	
3	4	pressure regulator	
2	8	manually operatet valve	
1	4	quick connect	
Nº	PTS	ITEM	MANUFACTURER

Stck. | Benennung | Zeichnung Nr. | Werkstoff (DIN) | Pos. Nr. | Abmessung, Lager-Nr. | DIN

elektrolytisch poliert ○ | relative Permeabilität ≤ 1,

Änderung

Passung | Abmaß | Datum | Name

Gez. | Bearb. | Gepr.

Maßstab

Max-Planck-Institut für Plasmaphysik
8046 Garching bei München

Bearb. | Tel.

PELLET GAS SUPPLY

3J-1EH-1077

Ersatz für

Ersetzt durch

Stückl. Nr.

Fig. 21 Pellet gas supply

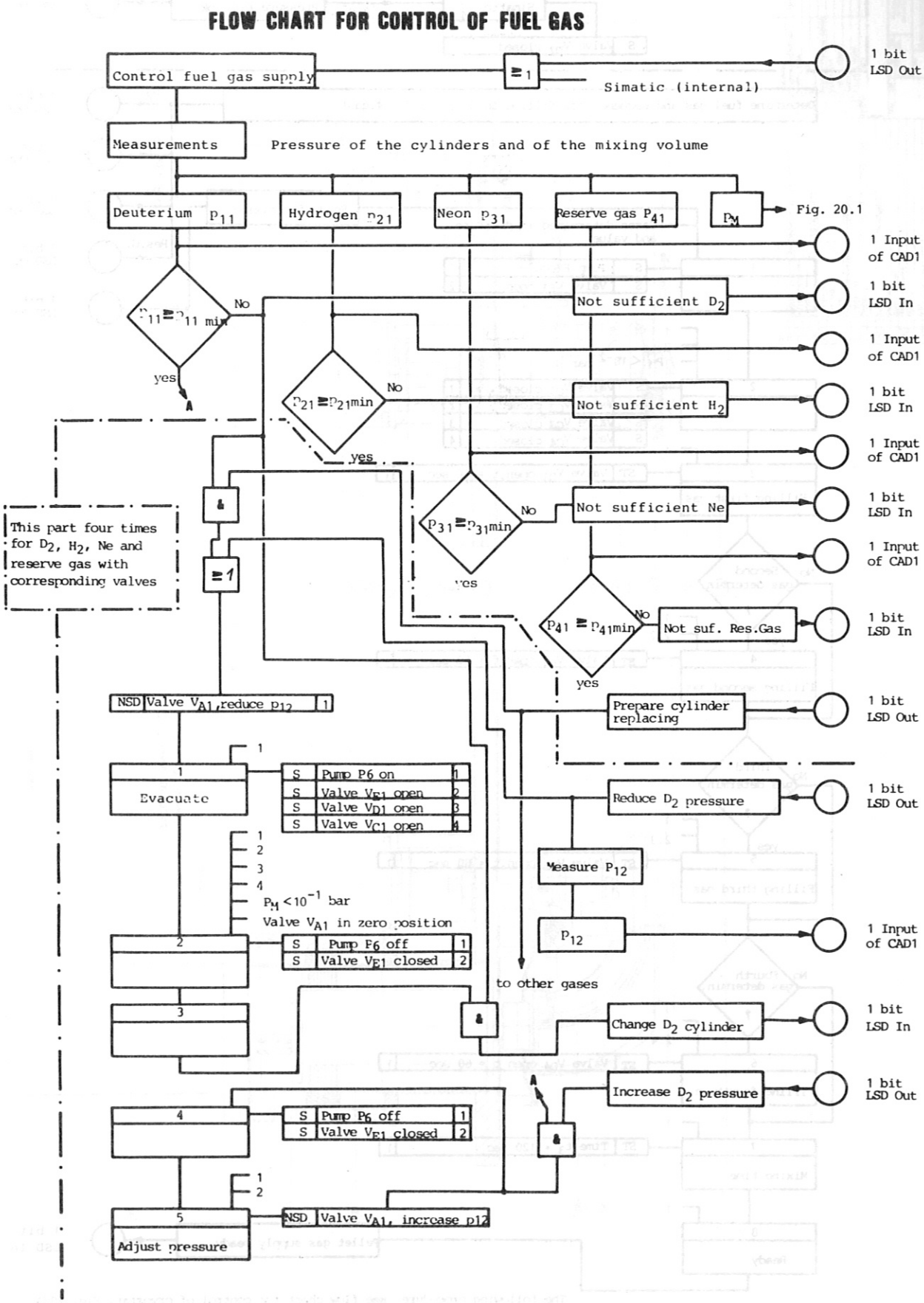

Fig. 22/1 Flow chart for control of fuel gas supply

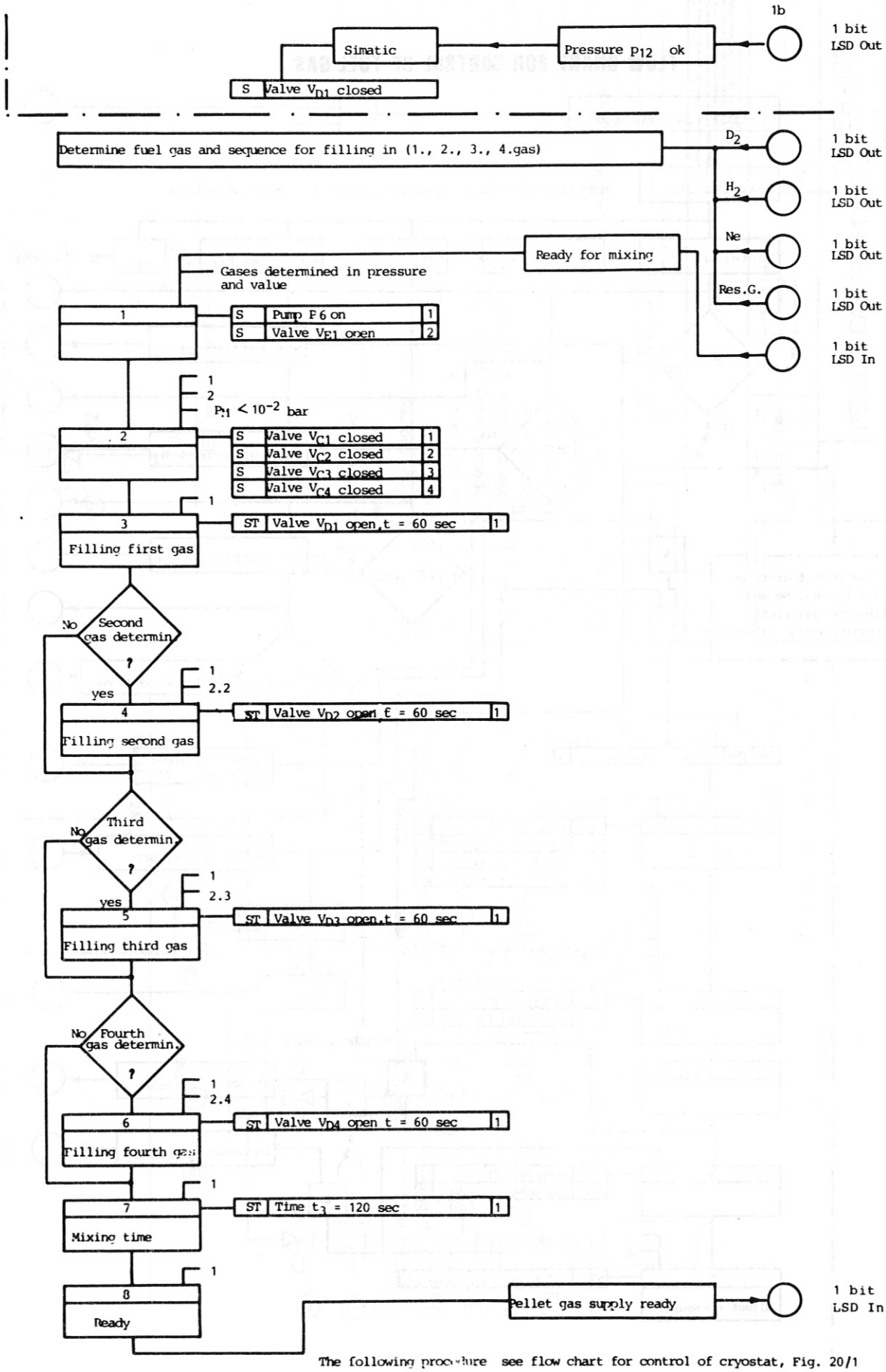

Fig. 22/2 Flow chart for control of fuel gas supply

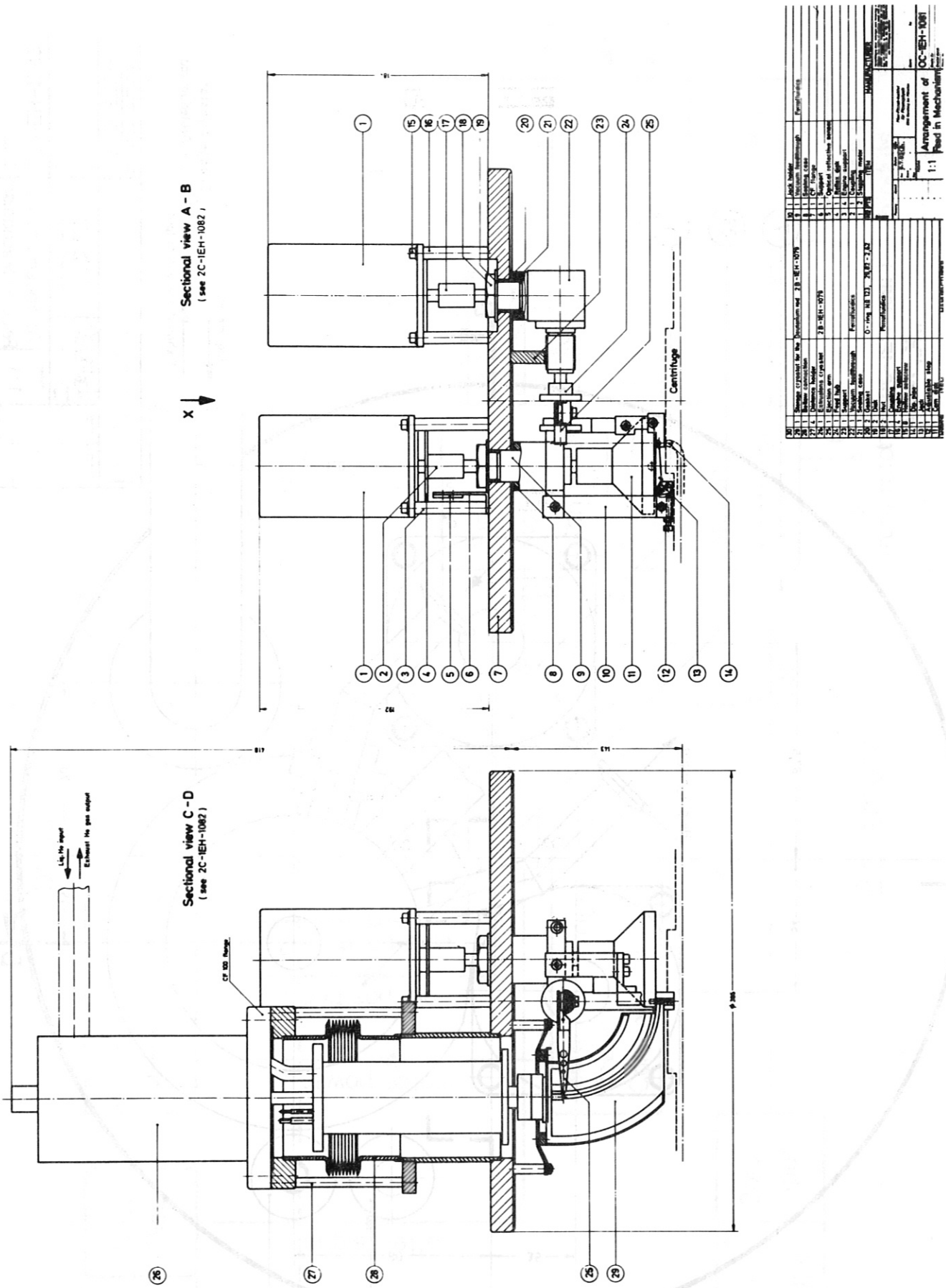

Fig. 23/1 Arrangement of feed-in mechanism (side view)

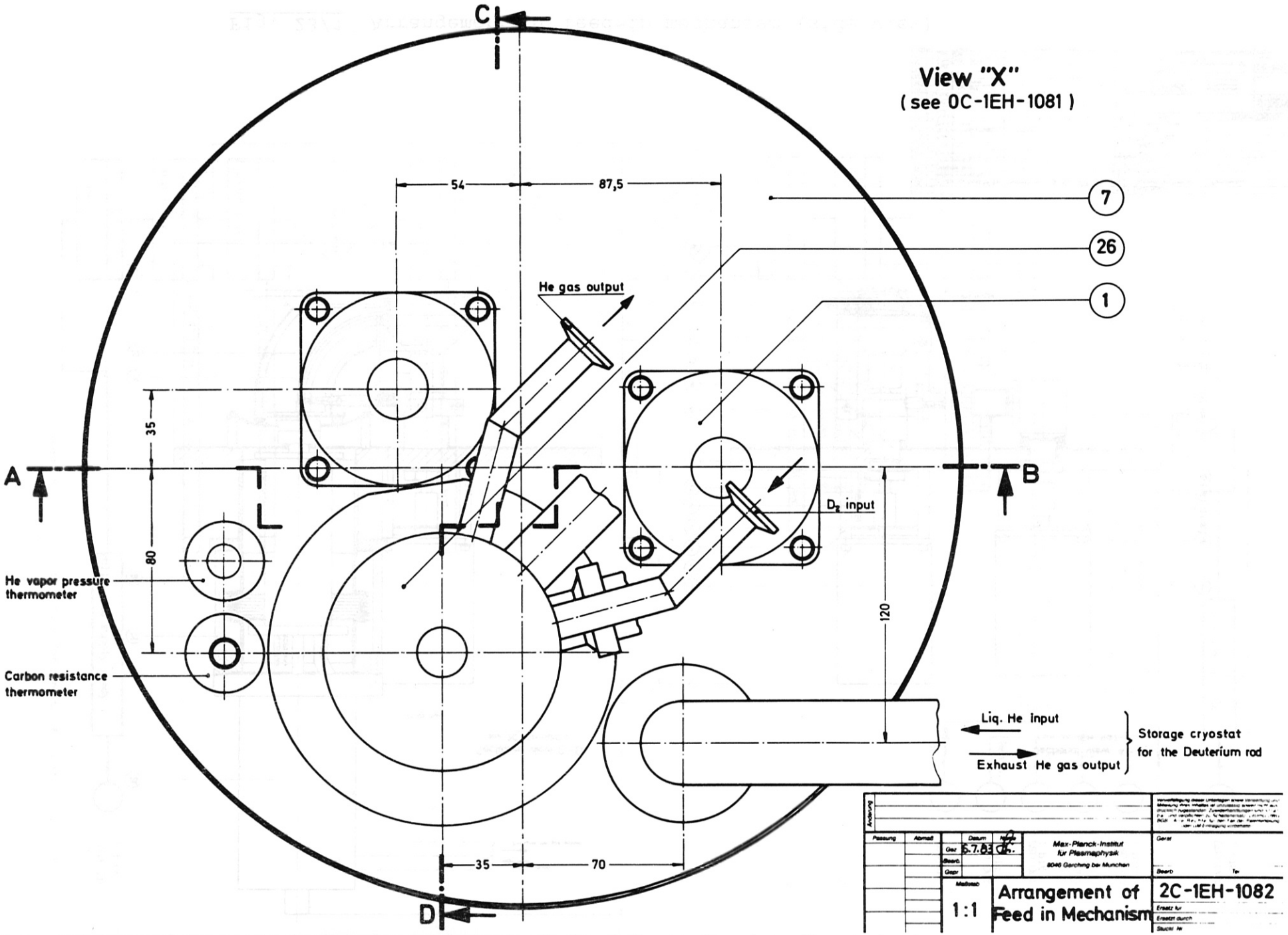

Fig. 23/2 Arrangement of feed-in mechanism (top view)

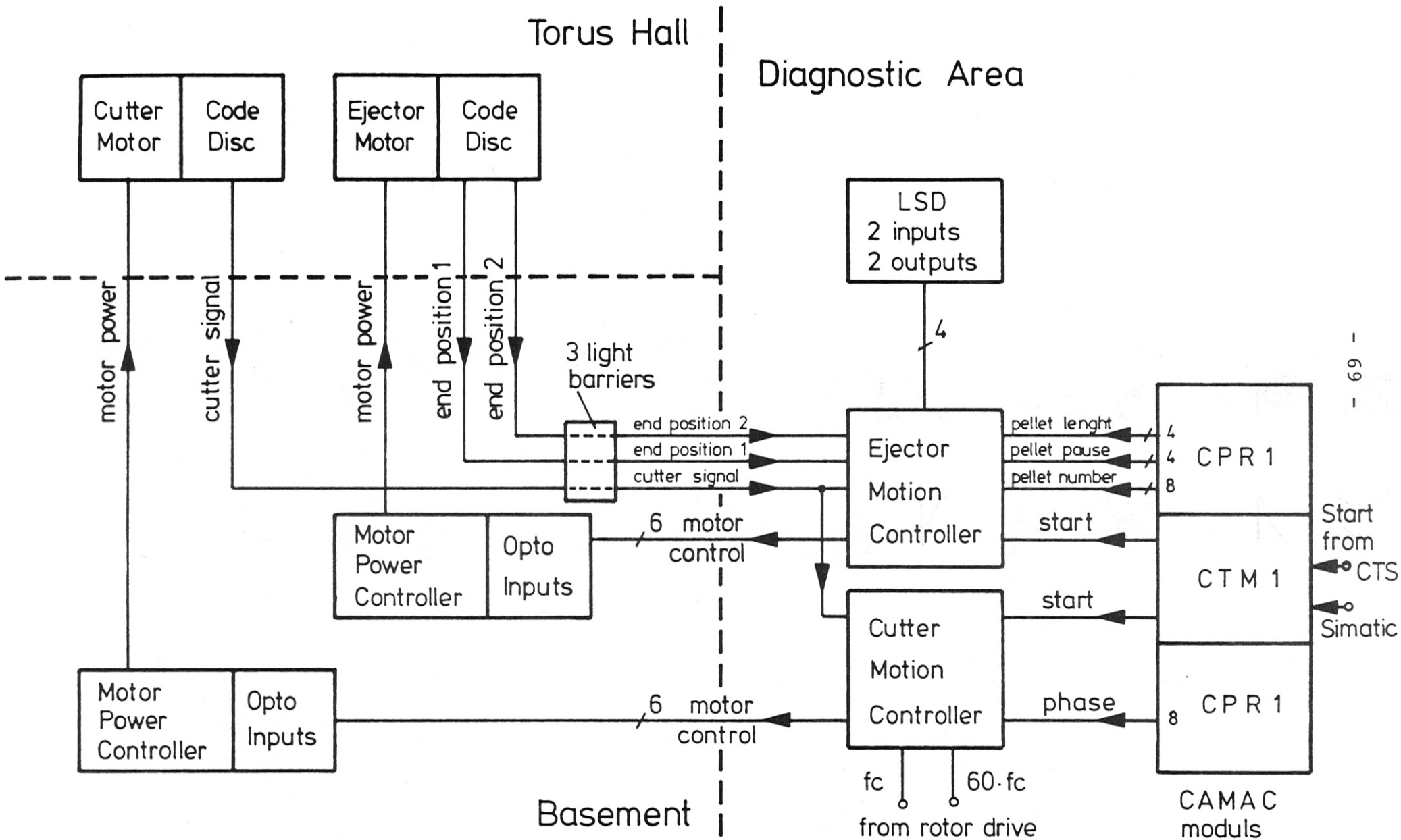

Fig. 24 Control and synchronization of pellet feed-in

Fig. 25 Photograph of test centrifuge

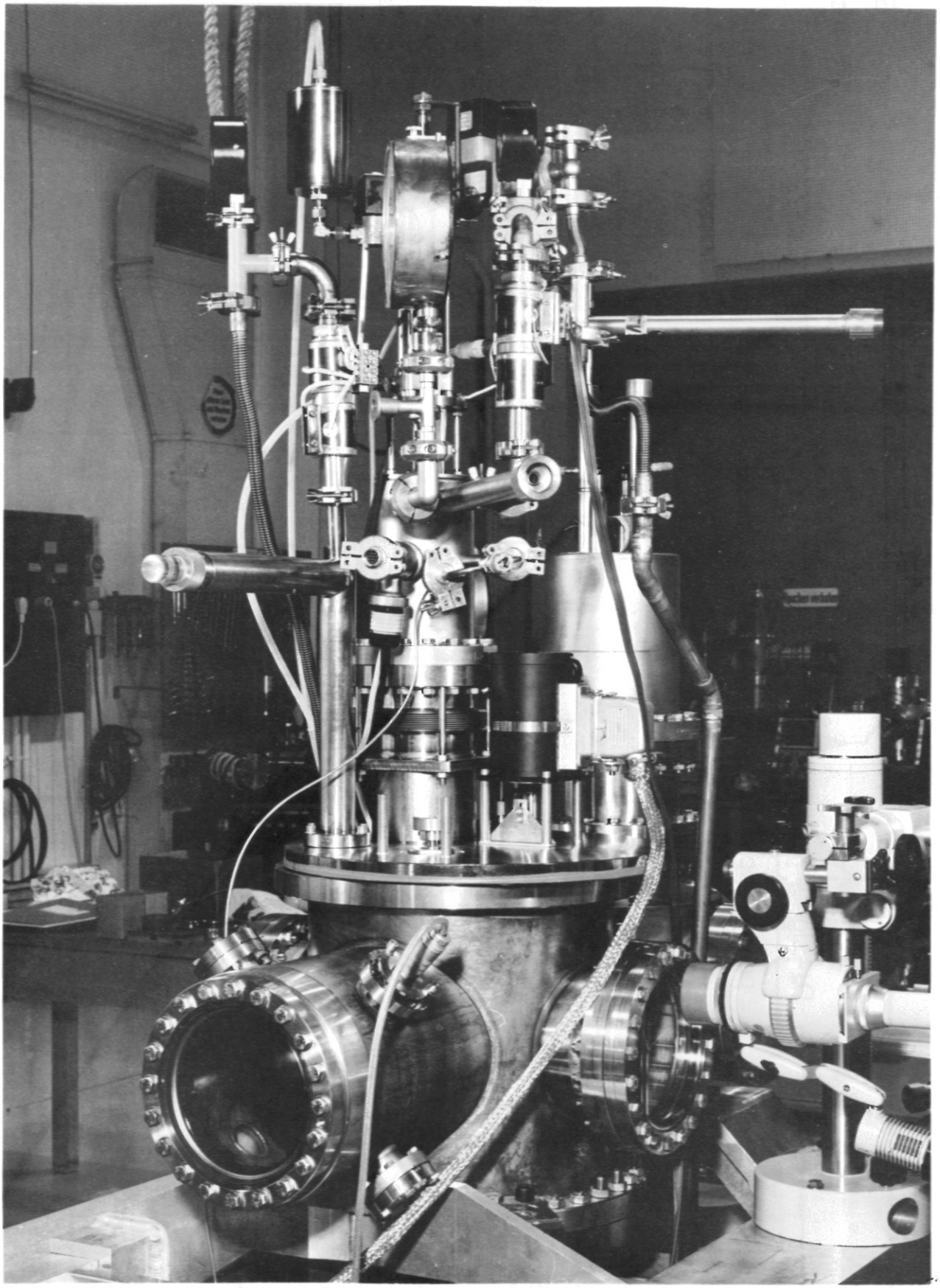

Fig. 26 Photograph of cryogenic test equipment

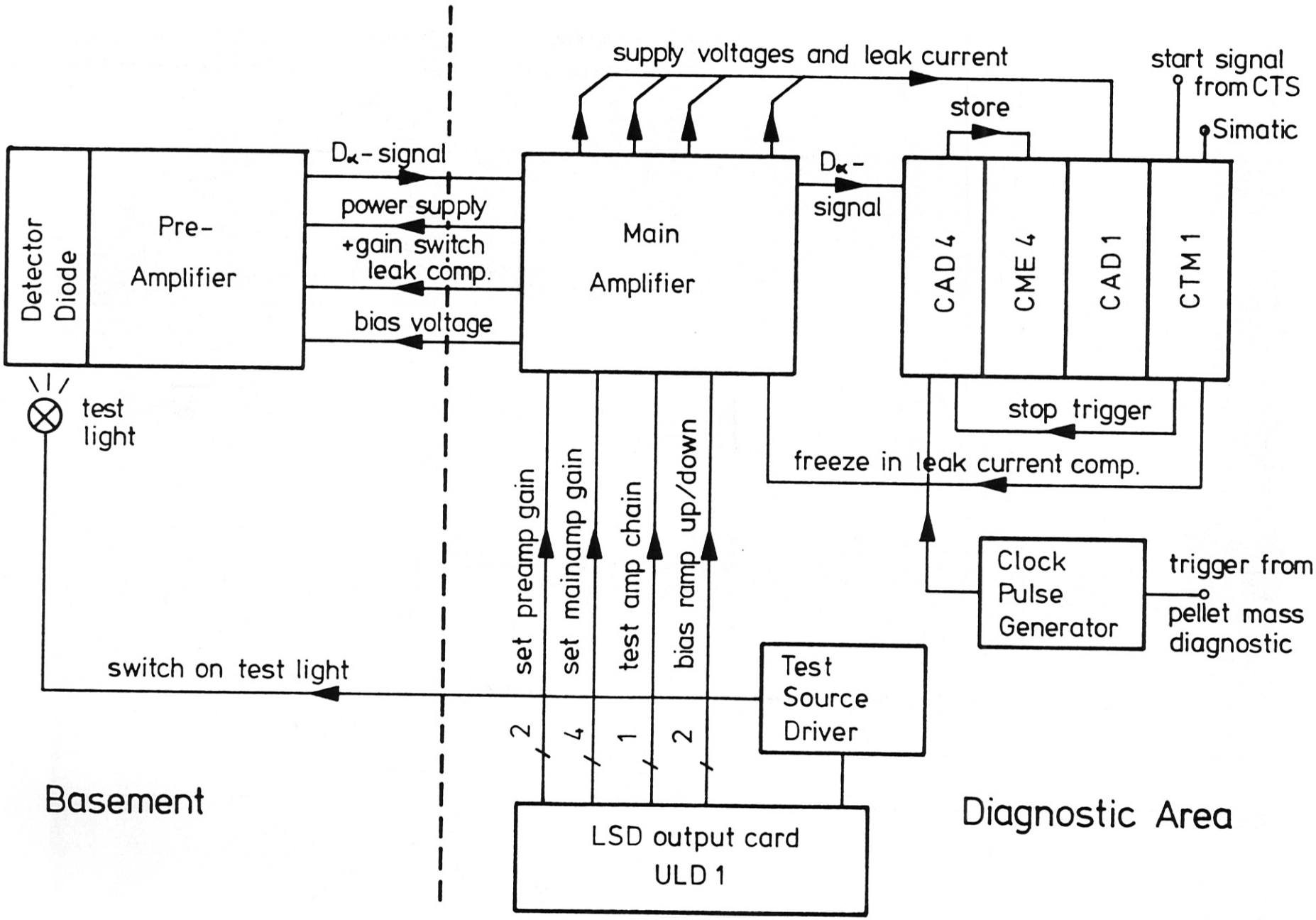

Fig. 27a Electronics for D α diagnostics

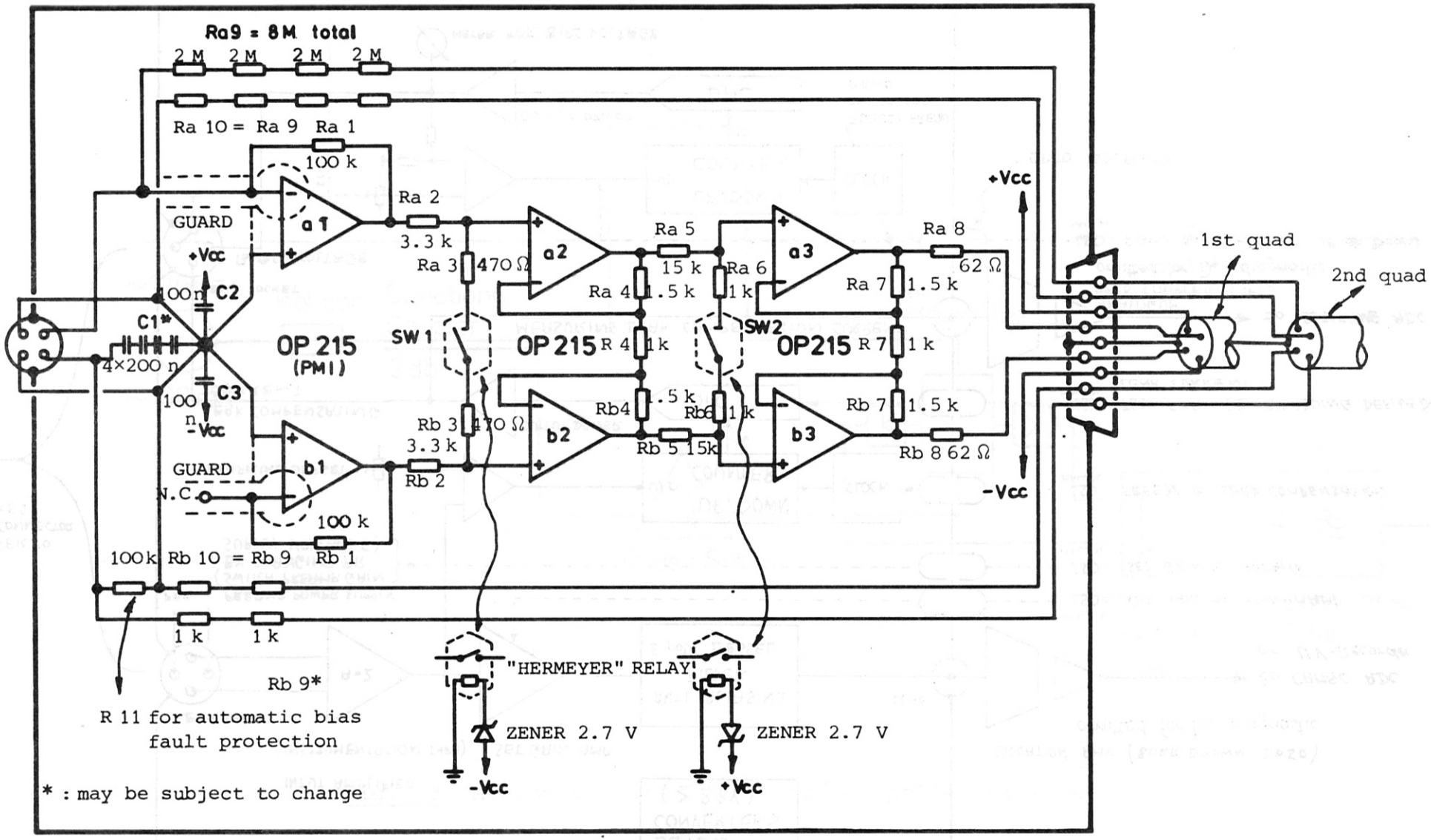

Fig. 27b Electronics for D_α diagnostics (preamplifier)

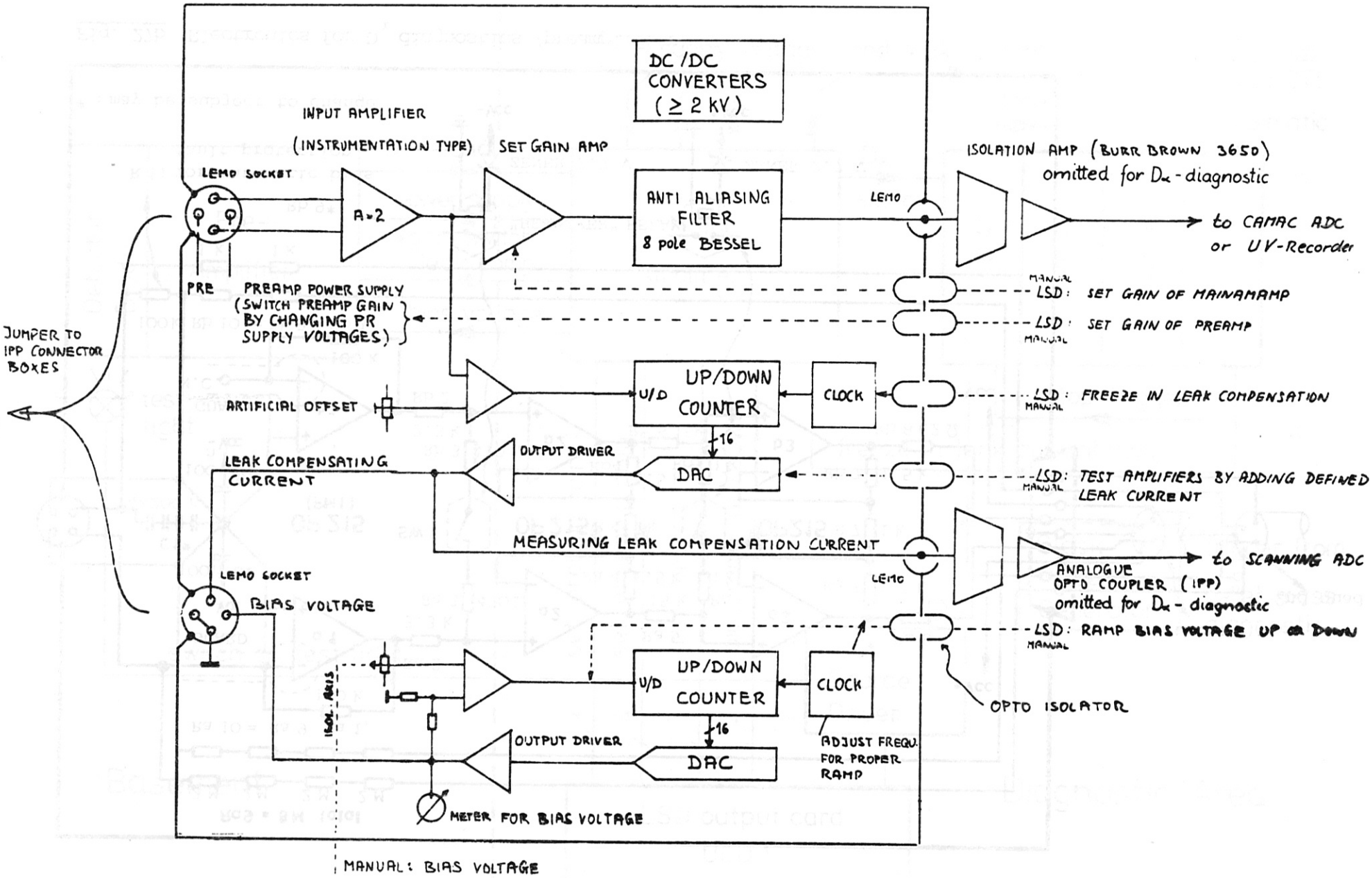

PROVISIONAL SOFT-X-RAY 'MAINAMP' 21-FEB-83/Sch.

Fig. 27c Electronics for Dα diagnostics (main amplifier)

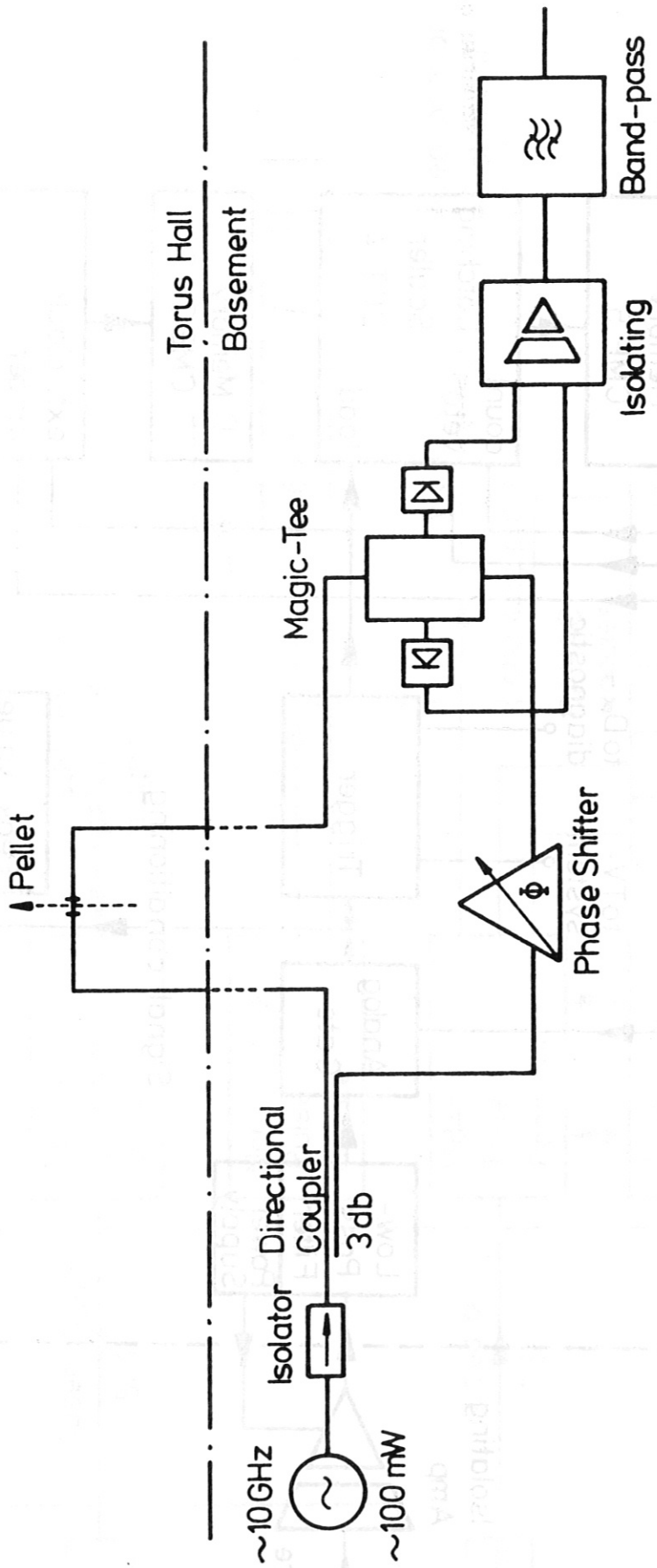

Fig. 28 Microwave interferometer for pellet mass determination

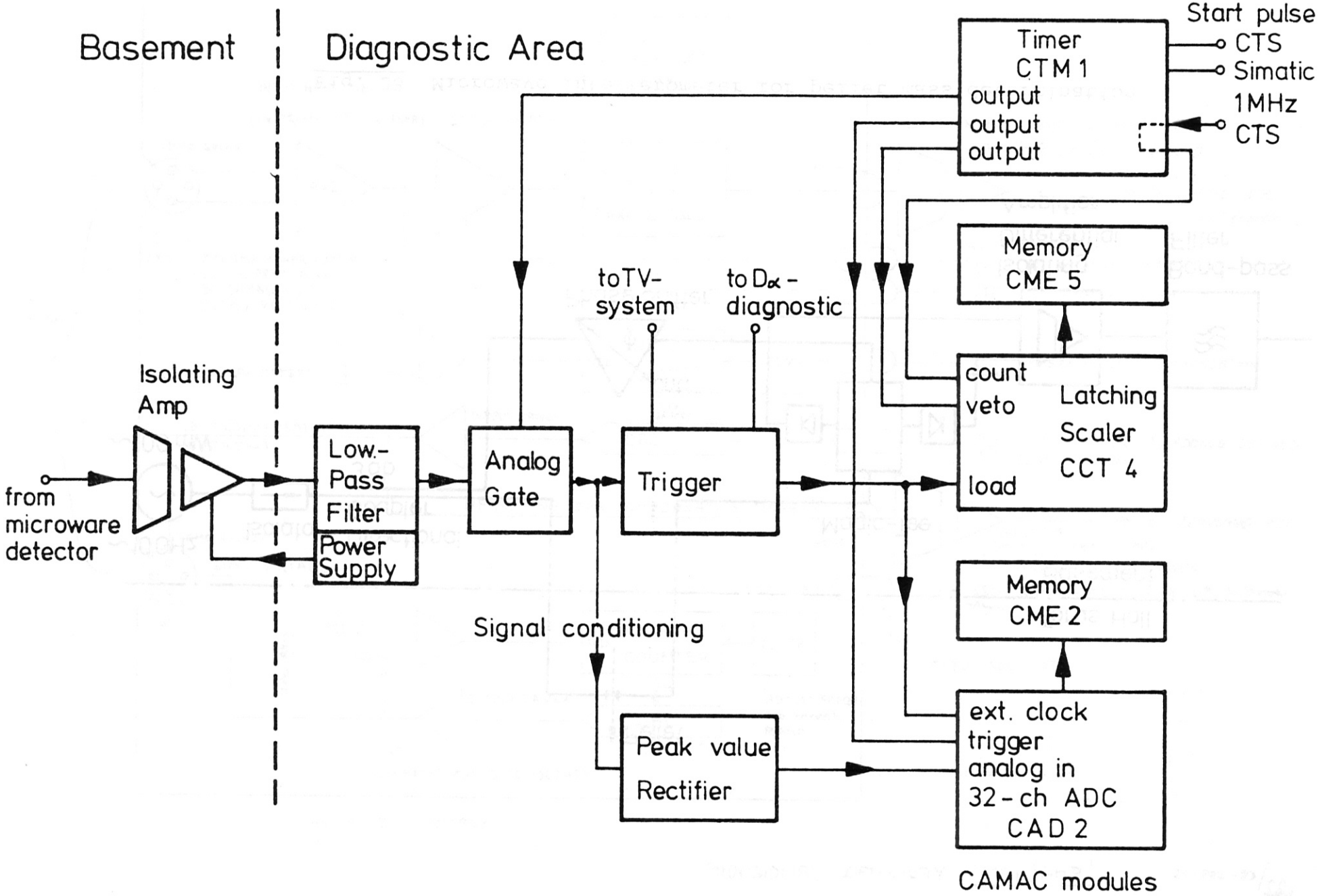

Fig. 29 Electronics for microwave interferometer

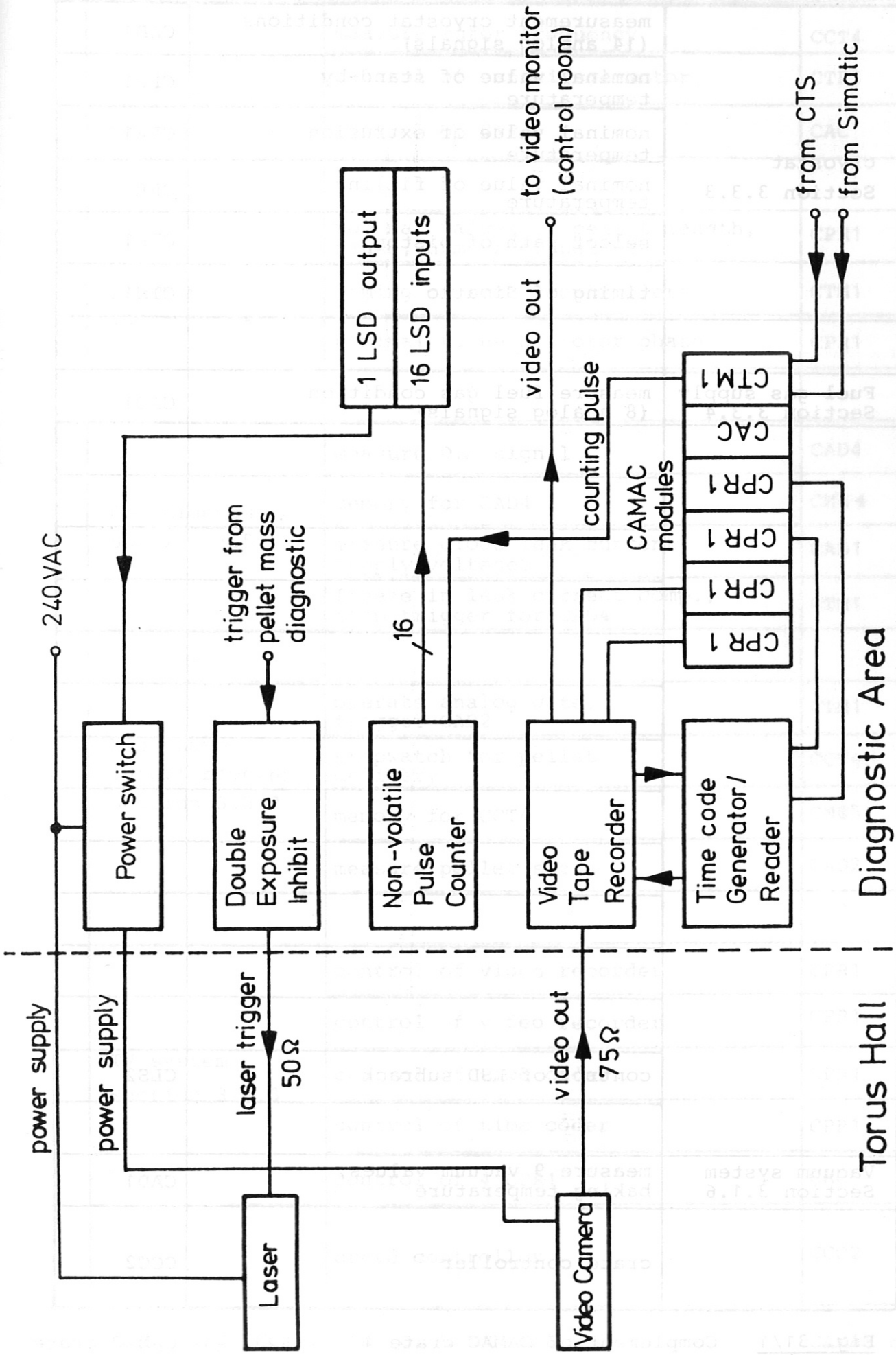

Fig. 30 TV pellet observation system

cryostat Section 3.3.3	measurement cryostat conditions (14 analog signals)	CAD1
	nominal value of stand-by temperature	CPR1
	nominal value of extrusion temperature	CPR1
	nominal value of filling temperature	CPR1
	select path of piston	CPR1
	timing of Simatic	CTM1
Fuel gas supply Section 3.3.4	measure fuel gas condition (8 analog signals)	CAD1
	control of LSD subrack	CLS2
Vacuum system Section 3.1.6	measure 9 vacuum values, baking temperature	CAD1
	crate controller	CCC2

Fig. 31/1 Complement of CAMAC crate 1

CAMAC crate CCB1

Rotor drive Section 3.2.4	measure rotor frequency	CCT4
	control of centrifuge motor	CTR3
	control of CTR3	CAC
Pellet feed-in Section 3.4.2	nominal values of pellet length, pause, number of pellets	CPR1
	timing of motor controllers	CTM1
	nominal value of rotor phase	CPR1
D_α diagnostic Section 3.5.1	measure D_α signal	CAD4
	memory for CAD4	CME 4
	measure diode leak current, supply voltages	CAD1
	freeze in leak current comp., stop trigger for CAD4	CTM1
Microwave interferometer Section 3.5.2	operate analog gate, trigger CAD2	CTM1
	stopwatch for pellet delivery	CCT4
	memory for CCT4	CME5
	measure pellet sizes	CAD2
TV system Section 3.5.3	control of video recorder	CPR1
	control of video recorder	CPR1
	control of time coder	CPR1
	control of time coder	CPR1
	control of 4 CPR1	CAC
	crate controller	CCC2

Fig. 31/2 Complement of CAMAC crate 2

CAMAC crate CCB1

cryostat Section 3.3.3	ULD2
	ULS1
Fuel gas supply Section 3.3.4	ULS1
	ULD2
	ULD2
Vacuum system Section 3.1.6	ULD2
	ULS1
	ULS1
Rotor drive Sec. 3.2.4 and Pellet feed-in Sec. 3.4.2	ULD2
	ULS1
D_α diagnostic Section 3.5.1 and TV system Section 3.5.3	ULD2
	ULS1
Connector card	ULC1
Power supply	UPS1

Fig. 31/3 Complement of LSD subrack

LSD subrack
ULB1